Friendly Jamming in a MIMO Wiretap Interference Network: A Nonconvex Game Approach

Peyman Siyari, *Student Member, IEEE,* Marwan Krunz, *Fellow, IEEE,* and Diep N. Nguyen, *Member, IEEE*

***Abstract*—We consider joint optimization of artificial noise (AN) and information signals in a MIMO wiretap interference network, wherein the transmission of each link may be overheard by several MIMO-capable eavesdroppers. Each information signal is accompanied with AN, generated by the same user to confuse nearby eavesdroppers. Using a noncooperative game, a distributed optimization mechanism is proposed to maximize the secrecy rate of each link. The decision variables here are the covariance matrices for the information signals and ANs. However, the nonconvexity of each link's optimization problem (i.e., best response) makes conventional convex games inapplicable, even to find whether a Nash Equilibrium (NE) exists. To tackle this issue, we analyze the proposed game using a relaxed equilibrium concept, called *quasi-Nash equilibrium* (QNE). Under a constraint qualification condition for each player's problem, the set of QNEs includes the NE of the proposed game. We also derive the conditions for the existence and uniqueness of the resulting QNE. It turns out that the uniqueness conditions are too restrictive, and do not always hold in typical network scenarios. Thus, the proposed game often has multiple QNEs, and convergence to a QNE is not always guaranteed. To overcome these issues, we modify the utility functions of the players by adding several specific terms to each utility function. The modified game converges to a QNE even when multiple QNEs exist. Furthermore, players have the ability to select a desired QNE that optimizes a given social objective (e.g., sum-rate or secrecy sum-rate). Depending on the chosen objective, the amount of signaling overhead as well as the performance of resulting QNE can be controlled. Simulations show that not only we can guarantee the convergence to a QNE, but also due to the QNE selection mechanism, we can achieve a significant improvement in terms of secrecy sum-rate and power efficiency, especially in dense networks.**

***Index Terms*—Wiretap interference network, MIMO, friendly jamming, quasi-Nash equilibrium, NE selection, nonconvex games.**

I. Introduction

PHYSICAL-layer (PHY-layer) security provides a cost-efficient alternative to cryptographic methods in scenarios where the use of the latter is either impractical or expensive. One of the common settings for PHY-layer security is the wiretap channel. In this channel, a node (Alice) wishes to transmit messages securely to a legitimate receiver (Bob) in the presence of one or more eavesdroppers (Eve). Most PHY-layer security techniques for the wiretap channel aim to improve information-theoretic secrecy, i.e., the *secrecy capacity*, defined as the largest amount of information that can be confidentially communicated between Alice and Bob.

Over the last decade, several PHY-layer security techniques have been proposed. Some of these techniques rely on the use of artificial noise (AN) as a friendly jamming (FJ) signal [1]. In this method, Alice uses multiple antennas to generate an FJ signal along with the information signal, increasing the interference at Eve but without affecting Bob. The authors in [1] proposed a simple version of this technique, which relies on MIMO zero-forcing to ensure that the FJ signal falls in the null-space of the channel between Alice and Bob. The interest in using AN for a single link is driven by pragmatic considerations, and not necessarily due to its optimality. In fact, it was shown in [2] that in one-Eve scenario, the optimal approach for securing a single link with the knowledge of Eve's location is not to use AN. Complementing the classic AN approach in [1], which relies on transmitting the AN in the null-space of the legitimate channel, it was shown in [3] that adding AN to both the legitimate channel and its null-space can further improve the secrecy rate of a link. In the case of multiple eavesdroppers, it was shown in [4] that the use of AN can significantly improve the secrecy rate compared to the case when AN is not used.

In a multi-link or network scenario, where several transmitters wish to convey their messages simultaneously to several legitimate receivers (see Fig. 1), the FJ signal of each transmitter must be designed to not interfere with other unintended (but legitimate) receivers in the network. This can be quite challenging when only limited or no coordination is possible between links. Therefore, providing PHY-layer secrecy has to be done in a distributed yet (ideally) noninterfering manner. Specifically, interference management for PHY-layer security involves two conflicting factors. On the one hand, the AN from one transmitter degrades the respective information signals at unintended (but legitimate) receivers. On the other hand, AN also increases the interference at eavesdroppers, and is hence useful in terms of improving the security of the communications.

The idea of using interference in networks to provide secrecy was discussed in [5]. The authors of [6] then considered a two-link SISO interference network. They showed that with a careful power control design for both links, one link can assist

Manuscript received May 3, 2016; revised September 30, 2016. Part of this paper was presented at IEEE GLOBECOM 2016. This research was supported in part by NSF (grants 1409172 and CNS-1513649), the Army research Office (grant W911NF-13-1-0302), the Qatar National Research Fund (grant NPRP 8-052-2-029), and the Australian Research Council (Discovery Early Career Researcher Award DE150101092). Any opinions, findings, conclusions, or recommendations expressed in this paper are those of the author(s) and do not necessarily reflect the views of NSF, ARO, QNRF, or ARC.

P. Siyari and M. Krunz are with the Department of Electrical and Computer Engineering, University of Arizona (e-mail:{psiyari, krunz}@email.arizona.edu).

Diep N. Nguyen is with the Faculty of Engineering and Information Technology, University of Technology Sydney, Australia (email: Diep.Nguyen@uts.edu.au).

the other in providing a rate demand guarantee as well as secure the transmission by increasing interference on a single-antenna eavesdropper. For the case of two transmitter-receiver-eavesdropper triples, the authors in [7] proposed a cooperative beamforming approach to achieve maximum secure degree of freedom for both users. In fact, given the knowledge of co-channel interference at the receivers, a cooperative transmission alignment scheme between transmitters is established such that their respective receivers will get interference-free signals and the eavesdropper corresponding to each link will receive interference. [6] and [7]. Note that both of these works consider only a two-user scenario, which limits their applicability. Specifically, in [6] one of the users generates only interference to provide PHY-layer security for the other user, so providing the PHY-layer secrecy of the former user is overlooked. Moreover, although [7] considers providing secrecy for both users (in a slightly different network than the one we consider), it requires a significant amount of signaling (i.e., coordination) between the two users. In this paper, we aim to provide PHY-layer security for all users while limiting the amount of coordination as much as possible.

We consider a peer-to-peer multi-link interference network in which we assume that the transmission of each link's information signal is accompanied with AN to blind possible eavesdroppers. Each node in the network is equipped with multiple antennas. Our goal is to design a framework through which the co-channel interference at each legitimate receiver is minimized while the aggregate interference at external eavesdroppers remains high. Because nodes cannot cooperate with each other in our settings, each link independently aims to maximize its secrecy rate by designing the covariance matrices (essentially, the precoders) of its information signal and AN. This independent secrecy optimization can be modeled under a game-theoretic framework in which the utility of each player (i.e., link) is his secrecy rate, and the player's strategy is to optimize the covariance matrices of information signal and AN. It turns out that finding the best response of each link requires solving a nonconvex optimization problem. Thus, the existence of a Nash Equilibrium (NE) cannot be proved using traditional concepts of convex (concave) games [8].

To tackle this challenge, we study this nonconvex game using a relaxed equilibrium concept called *quasi-Nash equilibrium* (QNE) [9]. A QNE is a solution of a variational inequality (VI) [10] obtained under the K.K.T optimality conditions of the players' problems. The concept of QNE has been recently used in [11] and [12] for sum-rate maximization in cognitive radio networks. In this work, for a MIMO wiretap interference network, we show that under a constraint qualification (CQ) condition for each player's problem, the set of QNEs also includes the NE. Sufficient conditions for the existence and uniqueness of the resulting QNE are provided. Then, an iterative algorithm is proposed to achieve the unique QNE.

Due to the noncoordination among links, the (Q)NEs of a purely noncooperative game often suffer from social-welfare loss (i.e., modest sum-utility like the secrecy sum-rate). Furthermore, the conditions that guarantee the uniqueness and convergence to the QNE are dependent on the channel state information (CSI) between links that is random, hence out of control. This forces the links to terminate their iterative optimizations at some point, resulting in a low secrecy sum-rate. To overcome this issue, we introduce an addition of a regularized term to the utility function of each player. These regularizations allow us to not only guarantee the convergence of the game, but also give links the ability to select a QNE of interest (among multiple QNEs) to converge to. We propose three possibilities for QNE selection, each providing different benefits and requiring a different amounts of communication overhead. The proposed QNE selection algorithm can improve the performance of the formerly proposed noncooperative game while keeping the communication overhead reasonably low. The major contributions of this paper are as follows:

- We propose a noncooperative game to model PHY-layer secrecy optimization in a multi-link MIMO wiretap interference network. Due to the nonconvexity of each player's optimization problem, the analysis of equilibria is done through the concept of QNE. We show that the set of QNEs includes NE as well.
- Because many network scenarios may involve multiple QNEs, the purely noncooperative games do not always guarantee the convergence to a unique QNE. Hence, we introduce the additional terms in the utility function of the players (in the proposed game) to guarantee the convergence to a QNE.
- We design mechanisms that allow us to select a QNE of a specific interest from multiple QNEs. QNE selection makes it possible to improve the resulting secrecy sum-rate of the modified game compared to a purely noncooperative game.
- We found out that managing the network interference (by both information signal and artificial noise) is more effective than aiming to increase the interference at eavesdroppers, in terms of improving the network secrecy sum-rate.

II. System Model

Consider the network shown in Fig. 1, where Q transmitters, $Q > 1$, communicate with Q corresponding receivers. The qth transmitter is equipped with N_{T_q} antennas, $q = 1, \ldots, Q$. The qth receiver has N_{R_q} antennas, $q = 1, \ldots, Q$. The link between each transmit-receive (Alice-Bob) pair may experience interference from the other $Q - 1$ links. There are K noncolluding Eves overhearing the communications. The kth Eve, $k = 1, \ldots, K$, has $N_{e,k}$ receive antennas[1]. The received signal at the qth receiver, $\mathbf{y}_q$, is

$$\mathbf{y}_q = \tilde{\mathbf{H}}_{qq}\mathbf{u}_q + \sum_{\substack{r=1 \\ r\neq q}}^{Q} \tilde{\mathbf{H}}_{rq}\mathbf{u}_r + \mathbf{n}_q, \ q \in \mathbb{Q} \tag{1}$$

where $\tilde{\mathbf{H}}_{rq}$ ($\tilde{\mathbf{H}}_{qq}$) denotes the $N_{R_q} \times N_{T_r}$ ($N_{R_q} \times N_{T_q}$) channel matrix between the rth (qth) transmitter and qth receiver, $\mathbf{u}_q$ is the $N_{T_q} \times 1$ vector of transmitted signal from the qth

[1]The treatment can be easily extended to colluding eavesdroppers by combining the K Eves into one with $\sum_{k=1}^{K} N_{e,k}$ antennas.

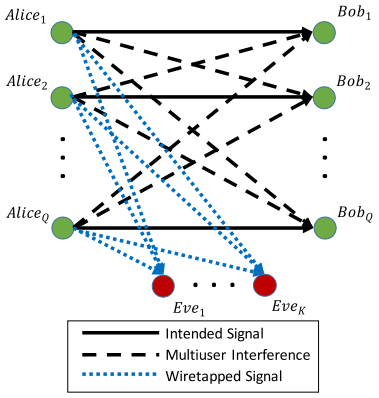

Fig. 1: System Model

transmitter, $\mathbf{n}_q$ is the $N_{R_q} \times 1$ vector of additive noise whose elements are i.i.d zero-mean circularly symmetric complex Gaussian distributed with unit variance, and $\mathbb{Q} \triangleq \{1, \ldots, Q\}$. The term $\sum_{\substack{r=1 \\ r \neq q}}^{Q} \tilde{\mathbf{H}}_{rq} \mathbf{u}_r$ is the multi-user interference (MUI). The received signal at the kth eavesdropper, $\mathbf{z}_k$, is expressed as

$$\mathbf{z}_k = \sum_{q=1}^{Q} \mathbf{G}_{qk} \mathbf{u}_q + \mathbf{n}_{e,k}, \;\; k \in \mathbb{K} \tag{2}$$

where $\mathbf{G}_{qk}$ is the $N_{e,k} \times N_{T_q}$ channel matrix between the qth transmitter and the kth eavesdropper, $\mathbf{n}_{e,k}$ is the $N_{e,k} \times 1$ vector of additive noise at the kth eavesdropper, and $\mathbb{K} \triangleq \{1, \ldots, K\}$. The transmitted signal $\mathbf{u}_q$ has the following form:

$$\mathbf{u}_q \triangleq \mathbf{s}_q + \mathbf{w}_q \tag{3}$$

where $\mathbf{s}_q$ is the information signal and $\mathbf{w}_q$ is the AN. We use the Gaussian codebook for the information signal and the Gaussian noise for the AN. The matrices $\mathbf{\Sigma}_q$ and $\mathbf{W}_q$ indicate the covariance matrices of $\mathbf{s}_q$ and $\mathbf{w}_q$, respectively.

The qth link, $q \in \mathbb{Q}$, together with K eavesdroppers form a compound wiretap channel for which the achievable secrecy rate of the qth link is written as [13]:

$$R_q^{sec}(\mathbf{\Sigma}_q, \mathbf{W}_q) \triangleq C_q(\mathbf{\Sigma}_q, \mathbf{W}_q) - \max_{k \in \mathbb{K}} C_{e,q,k}(\mathbf{\Sigma}_q, \mathbf{W}_q), \;\; q \in \mathbb{Q} \tag{4}$$

where $C_q(\mathbf{\Sigma}_q, \mathbf{W}_q)$ is the information rate and $C_{e,q,k}(\mathbf{\Sigma}_q, \mathbf{W}_q)$ is the received rate at the kth eavesdropper, $k \in \mathbb{K}$, while eavesdropping on the qth link, $q \in \mathbb{Q}$. Specifically,

$$C_q(\mathbf{\Sigma}_q, \mathbf{W}_q) \triangleq \ln \left| \mathbf{I} + \mathbf{M}_q^{-1} \mathbf{H}_{qq} \mathbf{\Sigma_q} \mathbf{H}_{qq}^H \right| = \ln \left| \mathbf{M}_q + \mathbf{H}_{qq} \mathbf{\Sigma_q} \mathbf{H}_{qq}^H \right| + \ln \left| \mathbf{M}_q^{-1} \right| \tag{5}$$

where $\mathbf{M}_q \triangleq \mathbf{I} + \mathbf{H}_{qq} \mathbf{W}_q \mathbf{H}_{qq}^H + \sum_{\substack{r=1 \\ r \neq q}}^{Q} \mathbf{H}_{rq} \left(\mathbf{\Sigma}_r + \mathbf{W}_r \right) \mathbf{H}_{rq}^H$ and

$$C_{e,q,k}(\mathbf{\Sigma}_q, \mathbf{W}_q) \triangleq \ln \left| \mathbf{I} + \mathbf{M}_{e,q,k}^{-1} \mathbf{G}_{qk} \mathbf{\Sigma_q} \mathbf{G}_{qk}^H \right| = \ln \left| \mathbf{M}_{e,q,k} + \mathbf{G}_{qk} \mathbf{\Sigma_q} \mathbf{G}_{qk}^H \right| + \ln \left| \mathbf{M}_{e,q,k}^{-1} \right| \tag{6}$$

where $\mathbf{M}_{e,q,k} \triangleq \mathbf{I} + \mathbf{G}_{qk} \mathbf{W}_q \mathbf{G}_{qk}^H + \sum_{\substack{r=1 \\ r \neq q}}^{Q} \mathbf{G}_{rk} \left(\mathbf{\Sigma}_r + \mathbf{W}_r \right) \mathbf{G}_{rk}^H$. The term $\mathbf{M}_q$ is the covariance matrix of received interference at the qth receiver and $\mathbf{M}_{e,q,k}$ is the covariance matrix of interference received at the kth eavesdropper while eavesdropping on the qth link[2]. Notice that both $\mathbf{M}_q$ and $\mathbf{M}_{e,q,k}$ include the information signal and AN of other $Q-1$ links. Furthermore, we require $\text{tr}(\mathbf{\Sigma}_q + \mathbf{W}_q) \leq P_q$ for all $q \in \mathbb{Q}$, where tr(.) is the trace operator and P_q is a positive value that represents the amount of power available (for both information and AN signals) at the qth transmitter.

III. Problem Formulation

We assume that the qth link, $q \in \mathbb{Q}$, optimizes its information and AN signals (through their covariance matrices $\mathbf{\Sigma}_q$ and $\mathbf{W}_q$) to maximize its own secrecy rate. The dynamics of such interaction between Q links can be modeled as a noncooperative game where each player (i.e., link) uses his best strategy to maximize his own utility (i.e., secrecy rate) given the strategies of other players. The best response of each player can be found by solving the following optimization problem

$$\begin{aligned} \underset{\mathbf{\Sigma}_q, \mathbf{W}_q}{\text{maximize}} \;\; & R_q^{sec}(\mathbf{\Sigma}_q, \mathbf{W}_q) \\ \text{s.t.} \;\; & (\mathbf{\Sigma}_q, \mathbf{W}_q) \in \mathcal{F}_q, \;\; q \in \mathbb{Q} \end{aligned} \tag{7}$$

where $\mathcal{F}_q \triangleq \{(\mathbf{\Sigma}_q, \mathbf{W}_q) | \text{tr}(\mathbf{\Sigma}_q + \mathbf{W}_q) \leq P_q, \;\; \mathbf{\Sigma}_q \succeq 0, \;\; \mathbf{W}_q \succeq 0\}$ is the set of all Hermitian matrices $(\mathbf{\Sigma}_q, \mathbf{W}_q)$ that are positive semi-definite (i.e., $\mathbf{\Sigma}_q \succeq 0, \;\; \mathbf{W}_q \succeq 0$) and meet the link's power constraint.

Unfortunately, problem (7) is a nonconvex optimization problem. In the remainder of this section, we aim to find a tractable solution for this problem. To that end, we first mention the following identity for a positive definite matrix $\mathbf{M}_q$ of size N_{R_q} [14, Example 3.23]:

$$\ln |\mathbf{M}_q^{-1}| = f(\mathbf{S}^*) = \max_{\mathbf{S} \in \mathbb{C}^{N_{R_q} \times N_{R_q}}, \mathbf{S} \succeq 0} f(\mathbf{S}) \tag{8}$$

where $f(\mathbf{S}) \triangleq -\text{tr}(\mathbf{S}\mathbf{M}_q) + \ln |\mathbf{S}| + N_{R_q}$ and $\mathbf{S}^* \triangleq \mathbf{M}_q^{-1}$ is the solution to the most RHS of (8). Applying the reformulation in (8) to the term $\ln |\mathbf{M}_q^{-1}|$ in (5) and $\ln \left| \mathbf{M}_{e,q,k} + \mathbf{G}_{qk} \mathbf{\Sigma_q} \mathbf{G}_{qk}^H \right|$ in (6), (7) can be rewritten as

$$\begin{aligned} \underset{\mathbf{\Sigma}_q, \mathbf{W}_q, \mathbf{S}_q}{\text{maximize}} \;\; & f_q(\mathbf{\Sigma}_q, \mathbf{W}_q, \{\mathbf{S}_{q,k}\}_{k=0}^K), \\ \text{s.t.} \;\; & (\mathbf{\Sigma}_q, \mathbf{W}_q) \in \mathcal{F}_q, \;\; \mathbf{S}_{q,k} \succeq 0, \;\; q \in \mathbb{Q}, \;\; k \in \{0\} \cup K \end{aligned} \tag{9}$$

where $\{\mathbf{S}_{q,k}\}_{k=0}^K = [\mathbf{S}_{q,0}^T, \ldots, \mathbf{S}_{q,K}^T]^T$, and

$$f_q(\mathbf{\Sigma}_q, \mathbf{W}_q, \{\mathbf{S}_{q,k}\}_{k=0}^K) \triangleq \varphi_q(\mathbf{\Sigma}_q, \mathbf{W}_q, \mathbf{S}_{q,0}) - \max_{k \in \mathbb{K}} \varphi_{e,q,k}(\mathbf{\Sigma}_q, \mathbf{W}_q, \mathbf{S}_{q,k}) \tag{10a}$$

$$\varphi_q(\mathbf{\Sigma}_q, \mathbf{W}_q, \mathbf{S}_{q,0}) \triangleq -\text{tr}(\mathbf{S}_{q,0}\mathbf{M}_q) + \ln |\mathbf{S}_{q,0}| + N_{R_q} + \ln \left| \mathbf{M}_q + \mathbf{H}_{qq} \mathbf{\Sigma_q} \mathbf{H}_{qq}^H \right| \tag{10b}$$

$$\varphi_{e,q,k}(\mathbf{\Sigma}_q, \mathbf{W}_q, \mathbf{S}_{q,k}) \triangleq \text{tr}(\mathbf{S}_{q,k}(\mathbf{M}_{e,q,k} + \mathbf{G}_{qk} \mathbf{\Sigma_q} \mathbf{G}_{qk}^H)) - \ln |\mathbf{S}_{q,k}| - N_{e,k} - \ln |\mathbf{M}_{e,q,k}| \,. \tag{10c}$$

Problem (9) is still nonconvex with respect to (w.r.t) $(\mathbf{\Sigma}_q, \mathbf{W}_q, \{\mathbf{S}_{q,k}\}_{k=0}^K)$. However, it is easy to verify that prob-

[2]Specifically, while eavesdropping on a user, an eavesdropper is treating interference as additive (colored) noise.

lem (9) is convex w.r.t either $(\mathbf{\Sigma}_q, \mathbf{W}_q)$ or $\{\mathbf{S}_{q,k}\}_{k=0}^K$ (by checking its Hessian). A stationary point to problem (7) that satisfies its K.K.T optimality conditions then can be found by solving (9) sequentially w.r.t $(\mathbf{\Sigma}_q, \mathbf{W}_q)$ and $\{\mathbf{S}_{q,k}\}_{k=0}^K$ [4, Section IV-B]. Specifically, in one iteration, problem (9) is solved w.r.t only $\{\mathbf{S}_{q,k}\}_{k=0}^K$ to find an optimal solution $\{\mathbf{S}_{q,k}^*\}_{k=0}^K$. Next, with $\{\mathbf{S}_{q,k}^*\}_{k=0}^K$ plugged in (10a), the problem in (9) is optimized w.r.t $(\mathbf{\Sigma}_q, \mathbf{W}_q)$ to find an optimal solution $(\mathbf{\Sigma}_q^*, \mathbf{W}_q^*)$. This Alternating Optimization (AO) cycle continues until reaching a convergence point. The nth iteration of AO, i.e., $(\mathbf{\Sigma}_q^n, \mathbf{W}_q^n, \{\mathbf{S}_{q,k}^n\}_{k=0}^K)$, is as follows:

$$(\mathbf{\Sigma_q^n}, \mathbf{W_q^n}) = \arg \max_{(\mathbf{\Sigma}_q, \mathbf{W}_q) \in \mathcal{F}_q} f_q(\mathbf{\Sigma}_q, \mathbf{W}_q, \left\{\mathbf{S}_{q,k}^{n-1}\right\}_{k=0}^K) \quad (11a)$$

$$\mathbf{S}_{q,0}^n \triangleq \arg \max_{\mathbf{S}_{q,0} \succeq 0} \varphi_q(\mathbf{\Sigma}_q^n, \mathbf{W}_q^n, \mathbf{S}_{q,0}) = (\mathbf{M}_q^n)^{-1} = \left(\mathbf{I} + \mathbf{H}_{qq}\mathbf{W}_q^n\mathbf{H}_{qq}^H + \sum_{\substack{r=1 \\ r\neq q}}^{Q} \mathbf{H}_{rq}\left(\mathbf{\Sigma}_r^0 + \mathbf{W}_r^0\right)\mathbf{H}_{rq}^H\right)^{-1} \quad (11b)$$

$$\mathbf{S}_{q,k}^n \triangleq \arg \max_{\mathbf{S}_{q,k} \succeq 0} \varphi_{e,q,k}(\mathbf{\Sigma}_q^n, \mathbf{W}_q^n, \mathbf{S}_{q,k}) = \left(\mathbf{M}_{e,q,k}^n + \mathbf{G}_{qk}{\mathbf{\Sigma_q}}^n\mathbf{G}_{qk}^H\right)^{-1} = \left(\mathbf{I} + \mathbf{G}_{qk}(\mathbf{\Sigma}_q^n + W_q^n)\mathbf{G}_{qk}^H + \sum_{\substack{r=1 \\ r\neq q}}^{Q} \mathbf{G}_{rk}\left(\mathbf{\Sigma}_r^0 + \mathbf{W}_r^0\right)\mathbf{G}_{rk}^H\right)^{-1} \quad (11c)$$

where $\mathbf{\Sigma}_r^0$ and $\mathbf{W}_r^0$ (for $r \neq q$) denote the received interference components at the qth receiver prior to solving (9). Incorporating (11b) and (11c) in (11a), the solution to the convex problem (11a) can be found using a convex optimization solver. Notice that in (11b) and (11c), the users do not coordinate with each other in the middle of finding a stationary point for (9), for all $q \in \mathbb{Q}$. Hence, the terms $\mathbf{\Sigma}_r^0$ and $\mathbf{W}_r^0$, $r \neq q$ remain constant during the AO iterations. To solve problem (9) faster, the authors in [4] solved the smooth approximation of (7) based on the log-sum-exp inequality [14, chapter 3.1.5], which states that

$$\max\{a_1, \ldots, a_K\} \leq \frac{1}{\beta}\ln(\sum_{k=1}^K e^{\beta a_k}) \leq \max\{a_1, \ldots, a_K\} + \frac{1}{\beta}\ln K. \quad (12)$$

where $a_k \in \mathbb{R}$ and $\beta > 0$. Applying (12) to (4), we can write problem (7) as

$$\begin{aligned} \underset{\mathbf{\Sigma}_q, \mathbf{W}_q}{\text{maximize}} \ & \bar{R}_{s,q}(\mathbf{\Sigma}_q, \mathbf{W}_q) \\ \text{s.t.} \quad & (\mathbf{\Sigma}_q, \mathbf{W}_q) \in \mathcal{F}_q, \ q \in \mathbb{Q} \end{aligned} \quad (13)$$

where

$$\bar{R}_{s,q}(\mathbf{\Sigma}_q, \mathbf{W}_q) \triangleq C_q(\mathbf{\Sigma}_q, \mathbf{W}_q) - \frac{1}{\beta}\ln(\sum_{k=1}^K \exp\{\beta C_{e,q,k}(\mathbf{\Sigma}_q, \mathbf{W}_q)\}), \ q \in \mathbb{Q}. \quad (14)$$

Hence, we can do the same reformulation procedure taken in (9) to end up with the following smooth reformulation [4]:

$$\begin{aligned} \underset{\mathbf{\Sigma}_q, \mathbf{W}_q, \mathbf{S}_q}{\text{maximize}} \ & \bar{f}_q(\mathbf{\Sigma}_q, \mathbf{W}_q, \{\mathbf{S}_{q,k}\}_{k=0}^K), \\ \text{s.t.} \quad & (\mathbf{\Sigma}_q, \mathbf{W}_q) \in \mathcal{F}_q, \ \mathbf{S}_k \succeq 0, q \in \mathbb{Q}, k \in \mathbb{K} \end{aligned} \quad (15)$$

where

$$\bar{f}_q(\mathbf{\Sigma}_q, \mathbf{W}_q, \{\mathbf{S}_{q,k}\}_{k=0}^K) \triangleq \varphi_q(\mathbf{\Sigma}_q, \mathbf{W}_q, \mathbf{S}_{q,0}) - \frac{1}{\beta}\ln\Big(\sum_{k=1}^K e^{\beta\varphi_{e,q,k}(\mathbf{\Sigma}_q, \mathbf{W}_q, \mathbf{S}_{q,k})}\Big). \quad (16)$$

with φ_q and $\varphi_{e,q,k}$ defined in (10b) and (10c), respectively. Hence, the AO iteration in (11a) changes to

$$(\mathbf{\Sigma_q^n}, \mathbf{W_q^n}) = \arg \max_{(\mathbf{\Sigma}_q, \mathbf{W}_q) \in \mathcal{F}_q} \bar{f}_q(\mathbf{\Sigma}_q, \mathbf{W}_q, \left\{\mathbf{S}_{q,k}^{n-1}\right\}_{k=0}^K), \quad (17)$$

while $\left\{\mathbf{S}_{q,k}^{n-1}\right\}_{k=0}^K$ remain the same as (11b) and (11c)[3]. After plugging (11b) and (11c) into (17), the solution to (17) at the nth iteration is computed using the Projected Gradient (PG) algorithm. The lth iteration of PG algorithm while solving (17) is as follows.

$$\begin{pmatrix} \hat{\mathbf{\Sigma}}_q^{n,l+1} \\ \hat{\mathbf{W}}_q^{n,l+1} \end{pmatrix} = \mathtt{Proj}_{\mathcal{F}_q}\begin{pmatrix} \mathbf{\Sigma}_q^{n,l} + \alpha_l \nabla_{\mathbf{\Sigma}_q} \bar{f}_q^{n,l} \\ \mathbf{W}_q^{n,l} + \alpha_l \nabla_{\mathbf{W}_q} \bar{f}_q^{n,l} \end{pmatrix}, \quad (18)$$

$$\begin{pmatrix} \mathbf{\Sigma}_q^{n,l+1} \\ \mathbf{W}_q^{n,l+1} \end{pmatrix} = \begin{pmatrix} \mathbf{\Sigma}_q^{n,l} \\ \mathbf{W}_q^{n,l} \end{pmatrix} + \varepsilon_l \begin{pmatrix} \hat{\mathbf{\Sigma}}_q^{n,l+1} - \mathbf{\Sigma}_q^{n,l} \\ \hat{\mathbf{W}}_q^{n,l+1} - \mathbf{W}_q^{n,l} \end{pmatrix}, \quad (19)$$

where α_l and ε_l are step sizes that can be determined using Wolfe conditions for PG method [15]; $\mathtt{Proj}_{\mathcal{F}_q}$ is the projection operator to the set $\mathcal{F}_q$, which can be written as

$$\mathtt{Proj}_{\mathcal{F}_q}\begin{pmatrix} \tilde{\mathbf{\Sigma}} \\ \tilde{\mathbf{W}} \end{pmatrix} = \min_{\mathbf{W}, \mathbf{\Sigma} \in \mathcal{F}_q} ||\mathbf{W} - \tilde{\mathbf{W}}||_F^2 + ||\mathbf{\Sigma} - \tilde{\mathbf{\Sigma}}||_F^2; \quad (20)$$

and $(\nabla_{\mathbf{\Sigma}_q} \bar{f}_q^{n,l}, \nabla_{\mathbf{W}_q} \bar{f}_q^{n,l}) = \Big(\nabla_{\mathbf{\Sigma}_q} \bar{f}_q(\mathbf{\Sigma}_q^{n,l}, \mathbf{W}_q^{n,l}, \left\{\mathbf{S}_{q,k}^{n-1}\right\}_{k=0}^K), \nabla_{\mathbf{W}_q} \bar{f}_q(\mathbf{\Sigma}_q^{n,l}, \mathbf{W}_q^{n,l}, \left\{\mathbf{S}_{q,k}^{n-1}\right\}_{k=0}^K)\Big)$ where

$$\nabla_{\mathbf{\Sigma}_q} \bar{f}_q(\mathbf{\Sigma}_q^{n,l}, \mathbf{W}_q^{n,l}, \left\{\mathbf{S}_{q,k}^{n-1}\right\}_{k=0}^K) = \mathbf{H}_{qq}^H(\mathbf{M}_q^{n,l} + \mathbf{H}_{qq}\mathbf{\Sigma}_q^{n,l}\mathbf{H}_{qq}^H)^{-1}\mathbf{H}_{qq} - \sum_{k=1}^K \rho_{q,k}^{n,l}\mathbf{G}_{q,k}^H\mathbf{S}_{q,k}^{n-1}\mathbf{G}_{q,k}, \quad (21a)$$

$$\mathbf{M}_q^{n,l} = \mathbf{I} + \mathbf{H}_{qq}\mathbf{W}_q^{n,l}\mathbf{H}_{qq}^H + \sum_{\substack{r=1 \\ r\neq q}}^{Q} \mathbf{H}_{rq}\left(\mathbf{\Sigma}_r^0 + \mathbf{W}_r^0\right)\mathbf{H}_{rq}^H, \quad (21b)$$

$$\rho_{q,k}^{n,l} = \frac{e^{\beta\varphi_{e,q,k}(\mathbf{\Sigma}_q^{n,l}, \mathbf{W}_q^{n,l}, \mathbf{S}_{q,k}^{n-1})}}{\sum_{j=1}^K e^{\beta\varphi_{e,q,j}(\mathbf{\Sigma}_q^{n,l}, \mathbf{W}_q^{n,l}, \mathbf{S}_{q,j}^{n-1})}}, \quad (21c)$$

[3]As far as optimality is concerned, it is shown in [4] that in the single-user scenario, the limit point of AO iterations done using (17), (11b), and (11c) are very close to the solutions found from AO iterations done using (11a), (11b), and (11c).

$$\nabla_{\mathbf{W}_q}\bar{f}_q(\mathbf{\Sigma}_q^{n,l},\mathbf{W}_q^{n,l},\left\{\mathbf{S}_{q,k}^{n-1}\right\}_{k=0}^{K})=$$
$$\mathbf{H}_{qq}^H\Big((\mathbf{M}_q^{n,l}+\mathbf{H}_{qq}\mathbf{\Sigma}_q^{n,l}\mathbf{H}_{qq})^{-1}-\mathbf{S}_{q,0}^{n-1}\Big)\mathbf{H}_{qq}+$$
$$\sum_{k=1}^{K}\rho_{q,k}^{n,l}\mathbf{G}_{qk}^H\left((\mathbf{M}_{e,q,k}^{n,l})^{-1}-\mathbf{S}_{q,k}^{n-1}\right)\mathbf{G}_{qk}, \quad (21d)$$

$$\mathbf{M}_{e,q,k}^{n,l}=\mathbf{I}+\mathbf{G}_{qk}\mathbf{W}_q^{n,l}\mathbf{G}_{qk}^H+\sum_{\substack{r=1\\r\neq q}}^{Q}\mathbf{G}_{rk}\left(\mathbf{\Sigma}_r^0+\mathbf{W}_r^0\right)\mathbf{G}_{rk}^H. \quad (21e)$$

The projection in (20) can be efficiently computed according to [4, Fact 1]. We refer to the game where the actions of the players are defined by (15) as the proposed smooth game. Now that we have the response of each user, we can analyze the dynamics of the proposed smooth game.

A pseudo-code of the proposed smooth game mentioned so far is shown in Algorithm 1. As mentioned earlier, finding a stationary point for (15) for each user consists of two nested loops. The inner loop involves the gradient projection which is shown in (18) and (19) (i.e., the loop in Line 6 of Algorithm 1). Once the optimal solution to inner loop is found, one AO iteration is done by recalculating $\{\mathbf{S}_{q,k}\}_{k=0}^{K}$ according to (11b) and (11c) in the outer loop (i.e., Line 4). After the AO iterations converge to a stationary point, the users begin their transmissions using the computed precoders of information signal and AN[4]. Therefore, one round of this competitive secrecy rate maximization is done. Notice that according to Line 2, the players will be notified of actions of each other (i.e., recalculate the received interference) only after the AO iterations has converged[5]. The last round of the game will be the one where the convergence is reached.

Algorithm 1 Proposed Smooth Game

Initialize: $\mathbf{\Sigma}_q^{1,1}$, $\mathbf{W}_q^{1,1}$, $\text{tr}(\mathbf{\Sigma}_q^{1,1}+\mathbf{W}_q^{1,1})<P_q$, $\forall q\in\mathbb{Q}$

1: **repeat**
2: Each link q computes $\mathbf{M}_q$, $\mathbf{M}_{e,q,k}$, $\forall k\in\mathbb{K}$ locally
3: **for** q =1,...,Q **do**
4: **for** n = 1,... **do**
5: Compute $\mathbf{S}_{q,k}^{n-1}$, $k=0,\ldots,K$
6: **for** l = 1,... **do**
7: Compute $\varphi_{e,q,k}(\mathbf{\Sigma}_q^{n,l},\mathbf{W}_q^{n,l},\mathbf{S}_{q,k}^{n-1})$, $\mathbf{M}_q^{n,l}$, $\mathbf{M}_{e,q,k}^{n,l}$, $\forall(q,k)$
8: Compute $(\mathbf{\Sigma}_q^{n,l+1},\mathbf{W}_q^{n,l+1})$ using (18)-(21) % Use Wolfe conditions
9: **end for**
10: **end for**
11: **end for**
12: **until** Convergence to QNE

[4]Although the optimization of covariance matrices of information signal and AN has been taken into account so far, the precoders can be found using eigenvalue decomposition.

[5]Such procedure in Line 2 of Algorithm 1 also explains the reason why $\mathbf{W}_r^0$ and $\mathbf{\Sigma}_r^0$ in (11) and (21) remain constant during AO iterations.

IV. Existence and Uniqueness of the QNE

Before we begin to analyze the existence and uniqueness of the QNE, we review fundamentals of variational inequality theory as the basis of our analyses.

Variational Inequality Theory: Let $F:\mathcal{Q}\to\mathbb{R}^N$ be a vector-valued continuous real function, where $N>1$ and $\mathcal{Q}\subseteq\mathbb{R}^N$ is a nonempty, closed, and convex set. The variational inequality VI$(F,\mathcal{Q})$ is the problem of finding a vector x^* such that

$$(x-x^*)^TF(x^*)\geq 0,\quad \forall x\in\mathcal{Q}. \quad (22)$$

The relation between variational inequality and game theory is summarized in the following theorem:

Theorem 1. *[10, Chapter 2] Consider Q players in a noncooperative game with utility function $f_q(x)$ for the qth player (not to be confused with the f_q defined in* (9)*), where $x\in\mathcal{Q}$ and $x=[x_1,x_2,...,x_Q]^T$, x_q is the qth player's strategy, and $f_q(x)$ is concave w.r.t x_q for all q. The set $\mathcal{Q}$ is comprised of all strategy sets (i.e., $\mathcal{Q}=\prod_{q=1}^{Q}\mathcal{Q}_q$, where $\mathcal{Q}_q$ is the qth player's strategy set). Assuming the differentiability of $f_q(x)$ w.r.t x_q and that $\mathcal{Q}_q$ is a closed and convex set for all q, the vector x^* is the NE of the game if for $F(x)=[-\nabla_{x_1}f_1(x),-\nabla_{x_2}f_2(x),...,-\nabla_{x_Q}f_Q(x)]^T$ we have:*

$$(x-x^*)^TF(x^*)\geq 0,\quad \forall x\in\mathcal{Q}.$$

□

A. Variational Inequality in Complex Domain

The theory of VI mentioned in (22) assumes that $\mathcal{Q}\subseteq\mathbb{R}^n$. However, this assumption might not be of our interest because the strategies of the players in our proposed game are two complex matrices (i.e., $\mathbf{\Sigma}_q$ and $\mathbf{W}_q$). Therefore, an alternative definition for VI in complex domain is needed. We use the definitions derived by the authors in [16] to define VI in complex domain.

Minimum Principle in Complex Domain: Consider the following optimization

$$\begin{aligned}&\underset{\mathbf{Z}}{\text{minimize}} \quad f(\mathbf{Z})\\ &\text{s.t.} \quad \mathbf{Z}\in\mathcal{K}\end{aligned} \quad (23)$$

where $f:\mathcal{K}\to\mathbb{R}$ is convex and continuously differentiable on $\mathcal{K}$ where $\mathcal{K}\subseteq\mathbb{C}^{N'\times N}$, $N'>1$, and $N>1$. $X\in\mathcal{K}$ is an optimal solution to (23) if and only if we have [16, lemma23]

$$\langle\mathbf{Z}-\mathbf{X},\nabla_{\mathbf{Z}}f(\mathbf{X})\rangle\geq 0,\ \forall\mathbf{Z}\in\mathcal{K}. \quad (24)$$

where $\langle\mathbf{A},\mathbf{B}\rangle=\text{Re}\left(Tr\left(\mathbf{A}^H\mathbf{B}\right)\right)$.

1) VI in Complex Domain: Using the definition of minimum principle in complex domain, we can now define the VI problem in the domain of complex matrices. For a complex-valued matrix $F^{\mathbb{C}}(\mathbf{Z}):\mathcal{K}\to\mathbb{C}^{N'\times N}$ where $\mathcal{K}\subseteq\mathbb{C}^{N'\times N}$, the VI in the complex domain is the problem of finding a complex matrix $\mathbf{Y}$ such that the following is satisfied [16, Definition 25]

$$\left\langle\mathbf{Z}-\mathbf{Y},F^{\mathbb{C}}(\mathbf{Y})\right\rangle\geq 0,\ \forall\mathbf{Z}\in\mathcal{K}. \quad (25)$$

B. Analysis of QNE

According to [9], the QNEs are tuples that satisfy the K.K.T conditions of all players' optimization problems. Under a constraint qualification, stationary points of each player's optimization problem satisfy its K.K.T conditions. One intuition that can be given on the concept of QNE is as follows. QNE is point where no player has a incentive to unilaterally change his strategy because any change makes a player not satisfy the K.K.T conditions of his problem. This is in contrast with the definition of NE in which the lack of incentives at NE is because of losing optimality. Again, optimality and satisfying the K.K.T conditions are equivalent when players solve convex programs.

To begin the analysis of the QNE, we first show that the stationary point found using AO mentioned previously (i.e., Line 4-10 of Algorithm 1) satisfies the K.K.T conditions of (13).

Proposition 1. *For the qth link, $q \in \mathbb{Q}$, the stationary point found using AO (i.e., Line 4-10 of Algorithm 1) satisfies the K.K.T conditions of* (13).

Proof: See [17, Appendix A]. ∎

Now that the K.K.T optimality of the stationary point found by AO iterations is proved, we rewrite the K.K.T conditions of all players to a proper VI problem [9]. The solution(s) to the obtained VI is the QNE(s) of the proposed smooth game. For the proposed smooth game defined using (15), we can establish the following VI to characterize the QNE points. Let the QNE point be as follows

$$\mathbf{Y} = \{\mathbf{Y}_q\}_{q=1}^{Q} \triangleq [\mathbf{\Sigma}^T, \mathbf{W}^T]^T = \{[\mathbf{\Sigma}_q^T, \mathbf{W}_q^T]^T\}_{q=1}^{Q} \tag{26}$$

where $\{[\mathbf{\Sigma}_q^T, \mathbf{W}_q^T]^T\}_{q=1}^{Q} = [\mathbf{\Sigma}_1^T, \mathbf{W}_1^T, \mathbf{\Sigma}_2^T, \mathbf{W}_2^T, \ldots, \mathbf{\Sigma}_Q^T, \mathbf{W}_Q^T,]^T$. Also, let the function $F^{\mathbb{C}}(Z)$ denote

$$F^{\mathbb{C}} = F^{\mathbb{C}}(\mathbf{\Sigma}, \mathbf{W}, \mathbf{S}) = \left\{F_q^{\mathbb{C}}(\mathbf{\Sigma}_q, \mathbf{W}_q, \{\mathbf{S}_{q,k}\}_{k=0}^{K})\right\}_{q=1}^{Q} \triangleq \left\{\left[-(\nabla_{\mathbf{\Sigma}_q}\bar{f}_q)^T, -(\nabla_{\mathbf{W}_q}\bar{f}_q)^T\right]^T\right\}_{q=1}^{Q} \tag{27}$$

where the terms $\nabla_{\mathbf{\Sigma}_q}\bar{f}_q$ and $\nabla_{\mathbf{W}_q}\bar{f}_q$ are given in (21). Therefore, $\mathbf{Y}$ solves the system of inequalities established by $VI(F^{\mathbb{C}}, \mathcal{K})$ in (25), where $\mathcal{K} = \prod_{q=1}^{Q} \mathcal{F}_q$. Note that for a given response $\mathbf{\Sigma}_q$ and $\mathbf{W}_q$, the solutions of $\{\mathbf{S}_{q,k}\}_{k=0}^{K}$ are uniquely determined by (11b) and (11c) for all q. Hence, from now on, we assume that the values of $\{\mathbf{S}_{q,k}\}_{k=0}^{K}$ are already plugged into $F_q^{\mathbb{C}}\left(\mathbf{\Sigma}_q, \mathbf{W}_q, \{\mathbf{S}_{q,k}\}_{k=0}^{K}\right)$, so we drop the term $\{\mathbf{S}_{q,k}\}_{k=0}^{K}$ in the subsequent equations for notational convenience.

In order to show that the K.K.T conditions are valid necessary conditions for a stationary solution of (13), an appropriate CQ must hold [18]. In this paper, we use the Slater's constraint qualification [18] as the strategy set of each player is a convex set. Moreover, at NE (if it exists) all of the players use their best responses, i.e., each player has found the optimal solution to his optimization problem and will not deviate from that. Since the optimal solution for each player also satisfies the K.K.T conditions, then NE must be a QNE [9]. In fact, the set of QNEs includes the NE.

C. Existence and Uniqueness of the QNE

To begin our analysis in this part, we consider the VI described by (25), (26), and (27) again. In the case of the domain of $\mathbf{Z}$ being square complex matrices, the definition of VI in complex domain can be further simplified to achieve the same form of VI in the real case (i.e., (22)). More specifically, let $F^{\mathbb{C}}$ be a $2N \times N$ matrix and let $\text{vec}(F^{\mathbb{C}}) \triangleq [(F_1)^T, \ldots, (F_N)^T]^T$ denote a $2N^2 \times 1$ vector where $F_i \triangleq [F^{\mathbb{C}}(\mathbf{Z})]_{:,i},\ i = 1, \ldots, N$, denotes the vector corresponding to the ith column of $F^{\mathbb{C}}(\mathbf{Z})$. Furthermore, let $\text{vec}(\mathbf{Z}) = [[\mathbf{Z}]_{:,1}^T, \ldots, [\mathbf{Z}]_{:,N}^T]^T$ be the vector version of the complex matrix $\mathbf{Z}$. Hence, the vector version of the VI in complex domain can be expressed as

$$(\text{vec}(\mathbf{Z}) - \text{vec}(\mathbf{Y}))^H \text{vec}(F^{\mathbb{C}}(\mathbf{Y})) \geq 0,\ \forall \mathbf{Z} \in \mathcal{K}. \tag{28}$$

In order to further simplify the VI in complex domain to be completely identical to the real case, we define $F^{\mathbb{R}} \triangleq [\text{Re}\left\{\text{vec}(F^{\mathbb{C}})\right\}^T, \text{Im}\left\{\text{vec}(F^{\mathbb{C}})\right\}^T]^T$ and $\mathbf{Z}^{\mathbb{R}} \triangleq [\text{Re}\left\{\text{vec}(\mathbf{Z})\right\}^T, \text{Im}\left\{\text{vec}(\mathbf{Z})\right\}^T]^T$ where Re{...} and I{...} are the real and imaginary parts, respectively. Therefore, the real-vectorized representation of (25) can be written as

$$\left(\mathbf{Z}^{\mathbb{R}} - \mathbf{Y}^{\mathbb{R}}\right)^T (F^{\mathbb{R}}(\mathbf{Y}^{\mathbb{R}})) \geq 0,\ \forall \mathbf{Z}^{\mathbb{R}} \in \mathcal{K}^{\mathbb{R}},\ \text{where } \mathcal{K}^{\mathbb{R}} \subseteq \mathbb{R}^{2N^2}. \tag{29}$$

The vector form of (26) and (27) are as follows:

$$\text{vec}(\mathbf{Z}) = [\text{vec}(\bar{\mathbf{\Sigma}})^T, \text{vec}(\bar{\mathbf{W}})^T]^T = \left\{[\text{vec}(\bar{\mathbf{\Sigma}}_q)^T, \text{vec}(\bar{\mathbf{W}}_q)^T]^T\right\}_{q=1}^{Q} \tag{30}$$

$$\text{vec}(F^{\mathbb{C}}(\mathbf{Z})) = \left\{\left[\text{vec}(-\nabla_{\mathbf{\Sigma}_q}\bar{f}_q)^T, \text{vec}(-\nabla_{\mathbf{W}_q}\bar{f}_q)^T\right]^T\right\}_{q=1}^{Q}. \tag{31}$$

Hence, the vector form of the complex VI problem $VI(F^{\mathbb{C}}, \mathcal{K})$ can be written as (32), and the equivalent real-vectorized representation of the VI in (25) that complies with the definition in (22) can be determined as (33) where $m \triangleq \sum_{q=1}^{Q} 2N_{T_q}^2$. Note that the set of matrices $(\mathbf{\Sigma}_1, \ldots, \mathbf{\Sigma}_Q, \mathbf{W}_1, \ldots, \mathbf{W}_Q)$ that are in $\mathcal{K} = \prod_{q=1}^{Q} \mathcal{F}_q$ are the ones whose real-vectorized versions will be inside $\mathcal{K}^{\mathbb{R}}$. Now that the proposed smooth game is modeled as a real-vectorized VI, we can use the following theorem to prove the existence of the QNE.

Theorem 2. *The proposed smooth game, where the actions of each player is given by* (15) *admits at least one QNE.*

Proof: See [17, Appendix B]. ∎

The uniqueness of the QNE is discussed in the following theorem:

Theorem 3. *The proposed smooth game characterized by* (15) *has a unique QNE if*

$$\lambda_{q,\min} > \sum_{\substack{q=1 \\ q \neq l}}^{Q} |||D_{Z_l} F_q^{\mathbb{C}}(Z_q)|||_2,\ q \in \mathbb{Q} \tag{34}$$

where $\lambda_{q,\min}$ is the smallest eigenvalue of $D_{Z_q} F_q^{\mathbb{C}}(Z_q)$, and

$$\left([\text{vec}(\boldsymbol{\Sigma})^T, \text{vec}(\mathbf{W})^T]^T - [\text{vec}(\bar{\boldsymbol{\Sigma}})^T, \text{vec}(\bar{\mathbf{W}})^T]^T\right)^H \text{vec}(F^{\mathbb{C}}(\bar{\boldsymbol{\Sigma}}, \bar{\mathbf{W}})) \geq 0. \tag{32}$$

$$\left(\left[\boldsymbol{\Sigma}^{\mathbb{R}^T}, \mathbf{W}^{\mathbb{R}^T}\right] - \left[\bar{\boldsymbol{\Sigma}}^{\mathbb{R}^T}, \bar{\mathbf{W}}^{\mathbb{R}^T}\right]\right) F^{\mathbb{R}} \geq 0, \ \forall (\boldsymbol{\Sigma}^{\mathbb{R}}, \mathbf{W}^{\mathbb{R}}) \in \mathcal{K}^{\mathbb{R}}, \ \mathcal{K}^{\mathbb{R}} \subseteq \mathbb{R}^m. \tag{33}$$

$D_{Z_l} F_q^{\mathbb{C}}(Z_q) \triangleq \frac{\partial \ vec\left(F_q^{\mathbb{C}}(Z_q)\right)}{\partial \ vec(Z_l)^T}$, *for all* $q, l \in \mathbb{Q}^2$, *is defined as*

$$D_{Z_l} F_q^{\mathbb{C}}(Z_q) \triangleq \begin{bmatrix} D_{\boldsymbol{\Sigma}_l}(-\nabla_{\boldsymbol{\Sigma}_q} \bar{f}_q) & D_{\mathbf{W}_l}(-\nabla_{\boldsymbol{\Sigma}_q} \bar{f}_q) \\ D_{\boldsymbol{\Sigma}_l}(-\nabla_{\mathbf{W}_q} \bar{f}_q) & D_{\mathbf{W}_l}(-\nabla_{\mathbf{W}_q} \bar{f}_q) \end{bmatrix}. \tag{35}$$

Proof: See [17, Appendix C]. ∎

V. Analysis of the Proposed Game in the Presence of Multiple QNEs

A. On the Convergence of Algorithm 1

The conditions for the uniqueness of the QNE do not guarantee the convergence of Algorithm 1 to a (unique) QNE. Since the optimization of each player is nonconvex, only stationary points of players' utilities could be achieved. Hence, solving each player's optimization problem using AO does not necessarily lead to the best response of each player. This hinders us from proving the convergence of Algorithm 1. However, we verified the convergence via simulations. In this section, we present a slightly modified algorithm, namely, the gradient-response algorithm with proof of convergence. Furthermore, the gradient-response algorithm paves the way for further performance improvements introduced later in this paper.

B. Gradient-Response Algorithm

A solution to the VI in (33) can be characterized by the following iteration [10, Chapter 12]:

$$x^{(i+1)} = \Pi_{\mathcal{K}^{\mathbb{R}}}\left(x^{(i)} - \gamma F^{\mathbb{R}}(x^{(i)}, \{S_{q,k}^{(i)}\}_{k=0}^K)\right) \tag{36}$$

where $\Pi_{\mathcal{K}^{\mathbb{R}}}$ is the projection to set $\mathcal{K}^{\mathbb{R}}$, $x = \left[\boldsymbol{\Sigma}^{\mathbb{R}^T}, \mathbf{W}^{\mathbb{R}^T}\right]^T$, the superscript (i) is the number of iterations, and $\gamma = \text{diag}([\gamma_1, \ldots, \gamma_m]^T)$ is a diagonal matrix which indicates the step size that each player takes in the improving direction of his utility function. The solutions to $\{\mathbf{S}_{q,k}^{(i)}\}_{k=0}^K$ are as follows:

$$\mathbf{S}_{q,0}^{(i)} \triangleq (\mathbf{M}_q^{(i)})^{-1} = \left(\mathbf{I} + \mathbf{H}_{qq}\mathbf{W}_q^{(i)}\mathbf{H}_{qq}^H + \sum_{\substack{r=1 \\ r\neq q}}^{Q} \mathbf{H}_{rq}\left(\boldsymbol{\Sigma}_r^{(i-1)} + \mathbf{W}_r^{(i-1)}\right)\mathbf{H}_{rq}^H\right)^{-1}, \tag{37a}$$

$$\mathbf{S}_{q,k\neq 0}^{(i)} \triangleq \left(\mathbf{M}_{e,q,k}^{(i)} + \mathbf{G}_{qk}\boldsymbol{\Sigma}_{\mathbf{q}}{}^{(i)}\mathbf{G}_{qk}^H\right)^{-1} = \left(\mathbf{I} + \mathbf{G}_{qk}(\boldsymbol{\Sigma}_q^{(i)} + W_q^{(i)})\mathbf{G}_{qk}^H + \sum_{\substack{r=1 \\ r\neq q}}^{Q} \mathbf{G}_{rk}\left(\boldsymbol{\Sigma}_r^{(i-1)} + \mathbf{W}_r^{(i-1)}\right)\mathbf{G}_{rk}^H\right)^{-1} \tag{37b}$$

where (37b) holds for $k \neq 0$. It is easy to confirm that the iteration in (36) is a simplified version of the projection done by each user in (18) and (19). Notice that the only difference of the gradient-response algorithm, characterized by iteration in (36), from Algorithm 1 is that at each round of the gradient-response algorithm, a player only does one iteration of the PG method (i.e., (18)) and one iteration according to (37). The real-vectorized version of the gradient-response algorithm is shown in (36). Since the values of $\{\mathbf{S}_{q,k}^{(i)}\}_{k=0}^K$ are uniquely determined for a given $x^{(i)}$, we drop the term $\{\mathbf{S}_{q,k}^{(i)}\}_{k=0}^K$ from the argument of $F^{\mathbb{R}}$ for notational convenience.

Assuming that $F^{\mathbb{R}}$ is *strongly monotone* (with modulus $c_s/2$)[6] and *Lipschitz continuous* (with constant L)[7] w.r.t $(\boldsymbol{\Sigma}_q, \mathbf{W}_q)$, the convergence to a unique solution follows if $\gamma_{i'} = d < \frac{c_s}{L^2}, \ \forall i' = 1, \ldots, m$, where d is constant. Hence, the mapping $x \to \Pi_{\mathcal{K}^{\mathbb{R}}}\left(x - \gamma F^{\mathbb{R}}(x)\right)$ becomes a contraction mapping and the fixed points of this map are solutions of the VI in (33) [10, Chapter 12]. It turns out that sufficient conditions for the strong monotonicity of $VI(F^{\mathbb{R}}, \mathcal{K}^{\mathbb{R}})$ are in fact the same as the conditions derived in (34) for the uniqueness of the QNE[8]. Therefore, based on (36), a pseudo-code of the gradient-response algorithm is given in Algorithm 2. Note that the operation in Line 6 of Algorithm 2 is the same as the iteration in (36). In fact, since the set $\mathcal{K}^{\mathbb{R}}$ is a Cartesian product of players' strategies, the iteration in (36) can be easily converted back to its matrix form to have the iteration in (38) for each link: Notice that γ_q' is a diagonal matrix that can obtained by dividing the matrix γ into Q block-diagonal matrices. That is, with a slight abuse of notations, $\gamma = \text{diag}([\gamma_1, \ldots, \gamma_m]^T) = \gamma' = \text{diag}(\gamma_1', \ldots, \gamma_Q')$, $Q < m$. Therefore, the gradient response in (36) can be shown as an iteration that is done in each link, independent of other links. This is essentially a distributed implementation. The gradient-response algorithm is given in Algorithm 2.

Algorithm 2 Gradient-Response Algorithm

Initialize: $\boldsymbol{\Sigma}_q^{(1)}$, $\mathbf{W}_q^{(1)}$, $\text{tr}(\boldsymbol{\Sigma}_q^{(1)} + \mathbf{W}_q^{(1)}) < P_q$, $\forall q$

1: **repeat** % superscript (i) indicates the iterations starting from here
2: Compute $\mathbf{M}_q$, $\mathbf{M}_{e,q,k}$, $\forall (q,k) \in \mathbb{Q} \times \mathbb{K}$
3: Compute $\mathbf{S}_{q,k}^{(i)}$, $\forall (q,k) \in \mathbb{Q} \times \mathbb{K}$
4: Compute $\varphi_{e,q,k}(\boldsymbol{\Sigma}_q^{(i)}, \mathbf{W}_q^{(i)}, \mathbf{S}_{q,k}^{(i)})$, $\forall (q,k) \in \mathbb{Q} \times \mathbb{K}$
5: **for** q =1,...,Q **do**
6: Compute $(\boldsymbol{\Sigma}_q^{(i+1)}, \mathbf{W}_q^{(i+1)})$ using (38)
7: **end for**
8: **until** Convergence to QNE

[6]The notion of strong monotonicity is a basic definition in the topic of VI (see [17, Appendix A]).

[7]It can be seen from (18) and (19) that the power constraint of each user makes the variations of $\nabla_{\boldsymbol{\Sigma}_q} \bar{f}_q$ and $\nabla_{\mathbf{W}_q} \bar{f}_q$ bounded for all $q \in \mathbb{Q}$. Hence, $F^{\mathbb{R}}$ is Lipschitz continuous on $\mathcal{K}^{\mathbb{R}}$.

[8]More explanation can be found in [17, Appendix A].

$$\begin{pmatrix} \mathbf{\Sigma}_q^{(i+1)} \\ \mathbf{W}_q^{(i+1)} \end{pmatrix} = \mathtt{Proj}_{\mathcal{F}_q} \begin{pmatrix} \mathbf{\Sigma}_q^{(i)} + \gamma_q' \nabla_{\mathbf{\Sigma}_q} \bar{f}_q(\mathbf{\Sigma}_q^{(i)}, \mathbf{W}_q^{(i)}, \left\{\mathbf{S}_{q,k}^{(i)}\right\}_{k=0}^{K}) \\ \mathbf{W}_q^{(i)} + \gamma_q' \nabla_{\mathbf{W}_q} \bar{f}_q(\mathbf{\Sigma}_q^{(i)}, \mathbf{W}_q^{(i)}, \left\{\mathbf{S}_{q,k}^{(i)}\right\}_{k=0}^{K}) \end{pmatrix}, \forall q \in \mathbb{Q}. \tag{38}$$

The convergence point of Algorithm 2 is a QNE of the game where players' actions are defined by (15). Specifically, assume that for $i \to \infty$, the convergence point is denoted as $(\bar{\mathbf{\Sigma}}, \bar{\mathbf{W}})$. Hence, we have for all $q \in \mathbb{Q}$

$$\bar{\mathbf{S}}_{q,0} = \arg \max_{\mathbf{S}_{q,0} \succeq 0} \varphi_q(\bar{\mathbf{\Sigma}}_q, \bar{\mathbf{W}}_q, \mathbf{S}_{q,0}) \tag{39a}$$

$$\bar{\mathbf{S}}_{q,k} = \arg \max_{\mathbf{S}_{q,k} \succeq 0} \varphi_{e,q,k}(\bar{\mathbf{\Sigma}}_q, \bar{\mathbf{W}}_q, \mathbf{S}_{q,k}),\ k \neq 0. \tag{39b}$$

The solution of (39a) and (39b) is the same as (37a) and (37b) for $i \to \infty$. By plugging the solutions of (39a) and (39b) in $\nabla_{\mathbf{\Sigma}_q} \bar{f}_q(\bar{\mathbf{\Sigma}}_q, \bar{\mathbf{W}}_q, \{\mathbf{S}_{q,k}\}_{k=0}^{K})$ and $\nabla_{\mathbf{W}_q} \bar{f}_q(\bar{\mathbf{\Sigma}}_q, \bar{\mathbf{W}}_q, \{\mathbf{S}_{q,k}\}_{k=0}^{K})$, the convergence point of Algorithm 2 is a QNE of the proposed game. Overall, by using the gradient-response algorithm, the uniqueness of the QNE and $\gamma_{i'} = d < \frac{c_s}{L^2},\ \forall i' = 1, \ldots, m$ directly suggest the convergence of the iteration in (36). Hence, a separate proof for the convergence of Algorithm 2 is not needed.

The iteration proposed in (36) has two major issues. First, the Lipschitz constant of $F^{\mathbb{R}}(x)$ has to be known. Apart from being difficult to derive, the knowledge of Lipschitz constant requires a centralized computation. Second, the strong monotonicity of $F^{\mathbb{R}}$ cannot be always guaranteed. In fact, the conditions derived in (34) are very dependent on the channel gains and network topology. Hence, in most typical network scenarios, the inequality in (34) cannot be satisfied. This means that in some situations, the game might have more than one QNE. Consequently, the convergence of Algorithm 2 is in jeopardy. However, on the condition that $F^{\mathbb{R}}$ is *monotone*[9], which is a weaker condition than strong monotonicity, the ability to choose between multiple QNEs is possible. This means that the users are able to select the QNE that satisfies a certain design criterion, thus guaranteeing convergence in the case of multiple QNEs. Moreover, depending on the design criterion, the performance of the resulting QNE in terms of the achieved secrecy sum-rate can be improved. To do this, we first review the regularization methods proposed for VIs.

C. Tikhonov Regularization

The general idea of regularization techniques is to modify the players' utility functions such that the VI becomes strongly monotone (and hence easily solvable by using Algorithm 2), and the limit point of a sequence of solutions for the modified VI converges to some solution of the original VI. In Tikhonov regularization, the process of regularizing $\text{VI}(F^{\mathbb{R}}, \mathcal{K}^{\mathbb{R}})$ involves solving a sequence of VIs, where the following iteration is characterized for a given ϵ [10, chapter 12]:

$$x^{(i+1)} = \Pi_{\mathcal{K}^{\mathbb{R}}} \left(x^{(i)} - \gamma^T \left(F^{\mathbb{R}}(x^{(i)}) + \epsilon x^{(i)} \right) \right). \tag{40}$$

[9]See [17, Appendix A] to recall the difference between monotonicity and strong monotonicity.

The solution to (40) when $i \to \infty$ is denoted as $x(\epsilon)$. Given that $F^{\mathbb{R}}$ is monotone, solving a sequence of (strongly monotone) $\text{VI}(F^{\mathbb{R}}(x) + \epsilon x, \mathcal{K}^{\mathbb{R}})$'s while $\epsilon \to 0$ has a limit point, (i.e., $\lim_{\epsilon \to 0} x(\epsilon)$ exists) and that limit point is equal to least-norm solution of the $\text{VI}(F^{\mathbb{R}}, \mathcal{K}^{\mathbb{R}})$ [10, Theorem 12.2.3].

D. QNE Selection using Tikhonov Regularization

Generalizing the applicability of Tikhonov regularization, we are more interested in converging to the QNE that is more beneficial to the users. In our approach to QNE selection, we define benefit as when the selected QNE satisfies a particular design criterion. Let the set of solutions of $\text{VI}(F^{\mathbb{R}}, \mathcal{K}^{\mathbb{R}})$ be denoted as $\text{SOL}(F^{\mathbb{R}}, \mathcal{K}^{\mathbb{R}})$. We want to select the NE that minimizes a strongly convex[10] function $\Phi(x) : \mathcal{K}^{\mathbb{R}} \to \mathbb{R}$. In fact, the QNE selection satisfies the following design criterion[11]

$$\begin{aligned} \text{minimize} \quad & \Phi(x) \\ \text{s.t.} \quad & x \in \text{SOL}(F^{\mathbb{R}}, \mathcal{K}^{\mathbb{R}}). \end{aligned} \tag{42}$$

The optimization in (42) is convex because the monotonicity of $F^{\mathbb{R}}$ suggests that $SOL(F^{\mathbb{R}}, \mathcal{K}^{\mathbb{R}})$ is a convex set [10, Chapter 2]. The unique point that solves problem (42), is the solution to $\text{VI}(\nabla\Phi(x), \text{SOL}(F^{\mathbb{R}}, \mathcal{K}^{\mathbb{R}}))$. However, as there is no prior knowledge on $\text{SOL}(F^{\mathbb{R}}, \mathcal{K}^{\mathbb{R}})$ (i.e., QNEs are not known), this optimization cannot be solved easily. To overcome this issue, we modify the function $F^{\mathbb{R}}$ in $\text{VI}(F^{\mathbb{R}}, \mathcal{K}^{\mathbb{R}})$ to

$$F_{\epsilon}^{\mathbb{R}} \triangleq F^{\mathbb{R}} + \epsilon \nabla \Phi(x). \tag{43}$$

As the function $\Phi(x)$ is a strongly convex function, its derivative w.r.t x is strongly monotone. Assuming that $F^{\mathbb{R}}$ is monotone, then the function $F_{\epsilon}^{\mathbb{R}}$ is strongly monotone and the solution to $\text{VI}(F_{\epsilon}^{\mathbb{R}}, \mathcal{K}^{\mathbb{R}})$, namely, $x(\epsilon)$, is unique for all values of $\epsilon > 0$ (i.e., convergence to a QNE can be guaranteed). Note that the iteration used for QNE selection is the same as (40) with the difference that the multiplier of ϵ in (40) is replaced by $\nabla\Phi(x)$. The following theorem shows the potential of using (43) in (36) for QNE selection:

Theorem 4. *[10, pp. 1128 and Theorem 12.2.5] Consider $\text{VI}(F_{\epsilon}^{\mathbb{R}}, \mathcal{K}^{\mathbb{R}})$ with $x(\epsilon)$ as its solution. Assume that $\mathcal{K}^{\mathbb{R}}$ is closed and convex, and $\text{SOL}(F^{\mathbb{R}}, \mathcal{K}^{\mathbb{R}})$ is nonempty. The following claims hold:*

- *The assumption that $\mathcal{K}^{\mathbb{R}}$ is closed and convex together with the nonemptiness of $\text{SOL}(F^{\mathbb{R}}, \mathcal{K}^{\mathbb{R}})$ (i.e., the existence of the QNE, proved in Theorem 2) are necessary and sufficient for $x_{\infty} = \lim_{\epsilon \to 0} x(\epsilon)$ to exist.*

[10]A strongly convex function is a function whose derivative is strongly monotone. We use the definitions of [19] to distinguish between different types of convexity.

[11]The discussion on how we determine the function $\Phi(x)$ will be tackled in Section VI-B.

$$x^{(i+1)} = \Pi_{\mathcal{K}^{\mathbb{R}}}\left(x^{(i)} - \gamma^{(i)}\left(F^{\mathbb{R}}(x^{(i)}) + \epsilon^{(j)}\nabla\Phi(x) + \theta^{(i)}(x^{(i)} - x^{(i-1)})\right)\right) \tag{41}$$

.

- *Assuming that $F^{\mathbb{R}}$ is monotone*[12]*, x_∞ is the solution of VI($\nabla\Phi(x), SOL(F^{\mathbb{R}}, \mathcal{K}^{\mathbb{R}})$). This means that a QNE among several QNEs can be selected*[13]. □

E. Distributed Tikhonov Regularization

Tikhonov regularization (QNE selection) is done in two nested loops. In the inner loop, for a given $\epsilon^{(j)}$, the solution to VI($F_\epsilon^{\mathbb{R}}, \mathcal{K}^{\mathbb{R}}$) will be found from the iteration in (40) (where the multiplier of ϵ is replaced with $\nabla\Phi(x)$). In the outer loop, the next value of $\epsilon^{(j)}$ will be chosen (according to a predefined sequence such that $\lim_{j\to\infty}\epsilon^{(j)} = 0$) until the solution to VI($\nabla\Phi(x)$, SOL($F^{\mathbb{R}}, \mathcal{K}^{\mathbb{R}}$)) is reached (cf. Theorem 4).

Despite having the ability to select a specific QNE among multiple QNEs, QNE selection requires heavy signaling and centralized computation because still the Lipschitz Continuity constant L and strong monotonicity modulus of $F_\epsilon^{\mathbb{R}}(x)$ must be known (cf. Section V-B). In order to address these issues, we introduce another regularization method, namely, proximal point regularization. In this regularization, a term $\theta^{(i)}(x^{(i)} - x^{(i-1)})$ is added to the function $F_\epsilon^{\mathbb{R}}(x)$ to build a function $F_{\epsilon,\theta}^{\mathbb{R}}(x) \triangleq F_\epsilon^{\mathbb{R}}(x) + \theta^{(i)}(x^{(i)} - x^{(i-1)})$ where $\theta^{(i)}$ is a diagonal matrix. Considering this modification, the following property can be used:

Proposition 2. *Let $F_\epsilon^{\mathbb{R}}(x)$ be a strictly monotone and Lipschitz continuous mapping*[14]*; $\max_{z\in\mathcal{K}^{\mathbb{R}}}||x|| \leq C$, and $\max_{z\in\mathcal{K}^{\mathbb{R}}}||F_\epsilon^{\mathbb{R}}|| \leq B$ where C and B are positive constants. Furthermore, suppose that for a given $\epsilon^{(j)}$, the solution to VI($F_\epsilon^{\mathbb{R}}, \mathcal{K}^{\mathbb{R}}$) is denoted as $x(\epsilon^{(j)})$. Let $x^{(i)}$ denote the set of iterates defined by* (41) *where the step size matrix $\gamma^{(i)}$ is changing with the iterations. Lastly, set $\gamma^{(i)}\theta^{(i)} = c = diag([c_1, \ldots, c_m])$ where $c_{i'} \in (0, 1), \forall i' = 1, \ldots, m$ is a constant, and let the following hold:*

$$\sum_{i=1}\gamma^{(i)} = \infty, \quad \sum_{i=1}^{\infty}\left(\gamma^{(i)}\right)^2 < \infty, \text{ and } \sum_{i=1}^{\infty}(\gamma_{max}^{(i)} - \gamma_{min}^{(i)}) < \infty. \tag{44}$$

where $\gamma_{max}^{(i)}$ and $\gamma_{min}^{(i)}$ are respectively the maximum and minimum diagonal elements of the matrix $\gamma^{(i)}$. Therefore, we have $\lim_{i\to\infty} x^{(i)} = x(\epsilon^{(j)})$. □

The proof of Proposition 2 can be found in [20, Proposition 3.4]. However, note that the assumption of strict monotonicity of $F_\epsilon^{\mathbb{R}}(x)$ is immediately satisfied as $F_\epsilon^{\mathbb{R}}(x)$ is already strongly monotone (cf. (43)). The conditions $\max_{z\in\mathcal{K}^{\mathbb{R}}}||x|| \leq C$ and $\max_{z\in\mathcal{K}^{\mathbb{R}}}||F_\epsilon^{\mathbb{R}}|| \leq B$ can also be satisfied due to having power constraints on each link. According to [20, Proposition 3.4], the step size $\gamma^{(i)}$ can be chosen as $\gamma_{i'}^{(i)} = (i + \alpha_{i'})^{-\omega}$, where $\alpha_{i'}$ is a positive integer for $i' = 1, \ldots, N$ and $0 < \omega < 1$. Hence, we can write

$$\gamma_{max}^{(i)} = (i + \alpha_{max})^{-\omega}, \quad \gamma_{min}^{(i)} = (i + \alpha_{min})^{-\omega}. \tag{45}$$

Note that in Proposition 2, $\theta^{(i)}$ is already set to $\theta^{(i)} = \frac{c}{\gamma^{(i)}}$. Using Proposition 2, we can design a distributed transmit optimization algorithm without the knowledge of Lipschitz constant and strong monotonicity modulus of $F_\epsilon^{\mathbb{R}}$. The next section discusses the implementation of QNE selection using (41)[15].

VI. The QNE Selection Algorithm: Design and Discussion

In this section of the paper, we propose the QNE selection algorithm together with three possible choices for the design criterion (i.e., $\Phi(x)$). Each of these choices imposes a certain amount of signaling overhead as well as a certain amount of improvement on the performance of Algorithm 1 and Algorithm 2.

A. QNE Selection Algorithm

The pseudo-code for the QNE selection algorithm is shown in Algorithm 3. As mentioned previously, it can be seen in Algorithm 3 that the modified game (i.e., QNE selection algorithm) is comprised of two nested loops: outer loop (i.e., Line 1), and inner loop (i.e., Line 3). In the outer loop, the jth member of $\epsilon^{(j)}$'s is selected. In the inner loop, the game is played among the players, and the players update their strategies according to (41). The sequence $\epsilon^{(j)}$ must be a decreasing sequence such that $\lim_{j\to\infty}\epsilon^{(j)} = 0$. The operation in Line 10 of Algorithm 3 can be written as (46). Notice that $\theta_q^{(i)}$ is a diagonal matrix that can obtained via dividing the matrix $\theta^{(i)}$ into Q block-diagonal matrices. That is, with a slight abuse of notations, $\theta^{(i)} = \text{diag}(\theta_1^{(i)}, \ldots, \theta_Q^{(i)})$. In the next subsection, we specifically explain the terms $\nabla_{\mathbf{\Sigma}_q}\Phi(x)$ and $\nabla_{\mathbf{W}_q}\Phi(x)$ in Line 10, so that Algorithm 3 will be completely defined. Lastly, notice that all of our analysis on VI problems were under the assumption that every player is solving a minimization problem as his strategy. Hence, if maximization is the strategy of each player, the proximal terms in (46) appear as a negative values. Furthermore, the addition of $\nabla_{\mathbf{\Sigma}_q}\Phi(x)$ and $\nabla_{\mathbf{W}_q}\Phi(x)$ means that $\Phi(x)$ must be a strongly concave function of x.

[12]We elaborate on the monotonicity assumption for $F^{\mathbb{R}}$ in [17, Section V].

[13]We emphasize that by QNE selection, the players are still maximizing their (modified) utility functions. Hence, the noncooperative nature of the game is still preserved.

[14]Note that Lipschitz continuity of $F_\epsilon^{\mathbb{R}}(x)$ requires both $F^{\mathbb{R}}(x)$ and $\nabla\Phi(x)$ to be Lipschitz continuous. Hence, the proposed choices for $\Phi(x)$ in the next section are all Lipschitz continuous.

[15]Note that in all of the proposed algorithms throughout this paper, it was assumed that at each round of the game, all of the players are maximizing the utilities. This update fashion is also known as Jacobi implementation. The feasibility of implementing the algorithms using other update fashions (e.g., Gauss-Seidel or Asynchronous) can be a subject of future research.

$$\begin{pmatrix} \mathbf{\Sigma}_q^{(i+1)} \\ \mathbf{W}_q^{(i+1)} \end{pmatrix} = \mathtt{Proj}_{\mathcal{F}_q} \left(\begin{array}{c} \mathbf{\Sigma}_q^{(i)} + \gamma_q' \left(\nabla_{\mathbf{\Sigma}_q} \bar{f}_q(\mathbf{\Sigma}_q^{(i)}, \mathbf{W}_q^{(i)}, \left\{ \mathbf{S}_{q,k}^{(i)} \right\}_{k=0}^{K}) + \epsilon^{(j)} \nabla_{\mathbf{\Sigma}_q} \Phi(x^{(i)}) - \theta_q^{(i)} (\mathbf{\Sigma}_q^{(i)} - \mathbf{\Sigma}_q^{(i-1)}) \right) \\ \mathbf{W}_q^{(i)} + \gamma_q' \left(\nabla_{\mathbf{W}_q} \bar{f}_q(\mathbf{\Sigma}_q^{(i)}, \mathbf{W}_q^{(i)}, \left\{ \mathbf{S}_{q,k}^{(i)} \right\}_{k=0}^{K}) + \epsilon^{(j)} \nabla_{\mathbf{W}_q} \Phi(x^{(i)}) - \theta_q^{(i)} (\mathbf{W}_q^{(i)} - \mathbf{W}_q^{(i-1)}) \right) \end{array} \right). \tag{46}$$

Algorithm 3 QNE Selection Algorithm

Initialize: $\mathbf{\Sigma}_q^{(1)}$, $\mathbf{W}_q^{(1)}$, $\mathrm{tr}(\mathbf{\Sigma}_q^{(1)} + \mathbf{W}_q^{(1)}) < P_q$, $\forall q$, and j = 1

repeat % Outer loop: superscript j indicates the iterations starting from here
  Choose the jth member of the sequence $\epsilon^{(j)}$
  repeat % Inner loop: superscript i indicates the iterations starting from here
    Compute $\mathbf{M}_q$, $\mathbf{M}_{e,q,k}$, $\forall (q,k) \in \mathbb{Q} \times \mathbb{K}$
    Compute $\mathbf{S}_{q,k}^{(i)}$, $\forall (q,k) \in \mathbb{Q} \times \mathbb{K}$
    Compute $\varphi_{e,q,k}(\mathbf{\Sigma}_q^{(i)}, \mathbf{W}_q^{(i)}, \mathbf{S}_{q,k}^{(i)})$, $\forall (q,k) \in \mathbb{Q} \times \mathbb{K}$
    for q = 1,...,Q **do**
    Replace $\nabla_{\mathbf{\Sigma}_q} \bar{f}_q$ with $\nabla_{\mathbf{\Sigma}_q} \bar{f}_q + \epsilon^{(j)} \nabla_{\mathbf{\Sigma}_q} \Phi(x^{(i)}) - \theta_q^{(i)} \left(\mathbf{\Sigma}_q^{(i)} - \mathbf{\Sigma}_q^{(i-1)} \right)$
    Replace $\nabla_{\mathbf{W}_q} \bar{f}_q$ with $\nabla_{\mathbf{W}_q} \bar{f}_q + \epsilon^{(j)} \nabla_{\mathbf{W}_q} \Phi(x^{(i)}) - \theta_q^{(i)} \left(\mathbf{W}_q^{(i)} - \mathbf{W}_q^{(i-1)} \right)$
    Compute $(\mathbf{\Sigma}_q^{(i+1)}, \mathbf{W}_q^{(i+1)})$ %Use (46)
    end for
  until Convergence to QNE % $x(\epsilon^j)$ is found.
  j = j+1
until Convergence to the limit point of $x(\epsilon^j)$'s

B. On the Choice of Design Criterion for QNE Selection

Assume that the derivatives of $\Phi(x)$ are described as:

$$\nabla \Phi(x) \triangleq [\nabla^{\mathbb{R}}_{\mathbf{\Sigma}_1, \mathbf{W}_1} \Phi(x)^T, \ldots, \nabla^{\mathbb{R}}_{\mathbf{\Sigma}_Q, \mathbf{W}_Q} \Phi(x)^T]^T, \tag{47a}$$

$$\nabla^{\mathbb{R}}_{\mathbf{\Sigma}_q, \mathbf{W}_q} \Phi(x) \triangleq [\nabla^{\mathbb{R}}_{\mathbf{\Sigma}_q} \Phi(x)^T, \nabla^{\mathbb{R}}_{\mathbf{W}_q} \Phi(x)^T]^T, \ q \in \mathbb{Q}, \tag{47b}$$

$$\nabla^{\mathbb{R}}_{\mathbf{\Sigma}_q} \Phi(x) \triangleq [\mathrm{Re}\{\mathrm{vec}(\nabla_{\mathbf{\Sigma}_q} \Phi(x))\}^T, \mathrm{Im}\{\mathrm{vec}(\nabla_{\mathbf{\Sigma}_q} \Phi(x))\}^T]^T, \tag{47c}$$

$$\nabla^{\mathbb{R}}_{\mathbf{W}_q} \Phi(x) \triangleq [\mathrm{Re}\{\mathrm{vec}(\nabla_{\mathbf{W}_q} \Phi(x))\}^T, \mathrm{Im}\{\mathrm{vec}(\nabla_{\mathbf{W}_q} \Phi(x))\}^T]^T. \tag{47d}$$

We are now ready to present the possible choices of $\Phi(x)$:

1) Maximizing the sum of information rates: We aim to select the QNE that maximizes the sum-rate of all links. Recalling the reformulated information rate (i.e., $\varphi_q(\mathbf{\Sigma}_q, \mathbf{W}_q, \mathbf{S}_{q,k})$) in (10b), $\Phi(x)$ can be described as (with $q \in \mathbb{Q}$):

$$\nabla_{\mathbf{\Sigma}_q} \Phi(x) = \sum_{\substack{r=1 \\ r \neq q}}^{Q} \mathbf{H}_{qr}^H \left((\mathbf{M}_r + \mathbf{H}_{rr} \mathbf{\Sigma}_r \mathbf{H}_{rr}^H)^{-1} - \mathbf{S}_{r,0} \right) \mathbf{H}_{qr}, \tag{48a}$$

$$\nabla_{\mathbf{W}_q} \Phi(x) = \sum_{\substack{r=1 \\ r \neq q}}^{Q} \mathbf{H}_{qr}^H \left((\mathbf{M}_r + \mathbf{H}_{rr} \mathbf{\Sigma}_r \mathbf{H}_{rr}^H)^{-1} - \mathbf{S}_{r,0} \right) \mathbf{H}_{qr}. \tag{48b}$$

Notice that although we wrote Φ as a function of x, one can easily relate the vector x to the covariance matrices $\{(\mathbf{\Sigma}_q, \mathbf{W}_q)\}_{q=1}^Q$ using (47) and (36). Hence, the derivatives of $\Phi(x)$ at the end of Algorithm 3 would be:

$$\nabla_{\mathbf{\Sigma}_q} \Phi(x) = \sum_{\substack{r=1 \\ r \neq q}}^{Q} \mathbf{H}_{qr}^H \left((\mathbf{M}_r^\star + \mathbf{H}_{rr} \mathbf{\Sigma}_r^\star \mathbf{H}_{rr})^{-1} - \mathbf{S}_{r,0}^\star \right) \mathbf{H}_{qr} \tag{49a}$$

$$\nabla_{\mathbf{W}_q} \Phi(x) = \sum_{\substack{r=1 \\ r \neq q}}^{Q} \mathbf{H}_{qr}^H \left((\mathbf{M}_r^\star + \mathbf{H}_{rr} \mathbf{\Sigma}_r^\star \mathbf{H}_{rr})^{-1} - \mathbf{S}_{r,0}^\star \right) \mathbf{H}_{qr} \tag{49b}$$

where $\mathbf{M}_r^\star = \mathbf{I} + \mathbf{H}_{rr}(\mathbf{W}_r^\star) \mathbf{H}_{rr}^H + \mathbf{H}_{qr}(\mathbf{W}_q^\star + \mathbf{\Sigma}_q^\star) \mathbf{H}_{qr}^H + \sum_{\substack{l=1 \\ l \neq q,r}}^{Q} \mathbf{H}_{lr} (\mathbf{\Sigma}_l^\star + \mathbf{W}_l^\star) \mathbf{H}_{lr}^H$, with $\mathbf{\Sigma}_q^\star$ and $\mathbf{W}_q^\star$ being the limit points of $\mathbf{\Sigma}_q$ and $\mathbf{W}_q$. Integrating (49a) w.r.t. $\mathbf{\Sigma}_q^\star$ and integrating (49b) w.r.t. $\mathbf{W}_q^\star$, we end up with $\Phi(x) = \sum_{q=1}^Q \sum_{\substack{r=1 \\ r \neq q}}^{Q} \varphi_r(\mathbf{\Sigma}_r, \mathbf{W}_r, \mathbf{S}_{r,0})$. Hence, at the end of Algorithm 3, the QNE that is a stationary point of sum-rate of all links is selected, i.e., the point that is the unique solution of $\mathrm{VI}(\nabla \Phi(x), \mathrm{SOL}(F^{\mathbb{R}}, \mathcal{K}^{\mathbb{R}}))$.

2) Minimizing the received rates at Eves: We can describe $\Phi(x)$ by (with $q \in \mathbb{Q}$)

$$\nabla_{\mathbf{\Sigma}_q} \Phi(x) = \sum_{\substack{r=1 \\ r \neq q}}^{Q} \sum_{k=1}^{K} \rho_{r,k} \mathbf{G}_{rk}^H \left((\mathbf{M}_{e,r,k}{}^{-1} - \mathbf{S}_{r,k}) \mathbf{G}_{rk} \right. \tag{50a}$$

$$\nabla_{\mathbf{W}_q} \Phi(x) = \sum_{\substack{r=1 \\ r \neq q}}^{Q} \sum_{k=1}^{K} \rho_{r,k} \mathbf{G}_{rk}^H \left((\mathbf{M}_{e,r,k}{}^{-1} - \mathbf{S}_{r,k}) \mathbf{G}_{rk} \right. \tag{50b}$$

$$\mathbf{M}_{e,r,k} \triangleq \mathbf{I} + \mathbf{G}_{rk} \mathbf{W}_r \mathbf{G}_{rk}^H + \mathbf{G}_{qk} (\mathbf{\Sigma}_q + \mathbf{W}_q) \mathbf{G}_{qk}^H + \tag{50c}$$

$$\sum_{\substack{l=1 \\ l \neq q,r}}^{Q} \mathbf{G}_{lk} (\mathbf{\Sigma}_l + \mathbf{W}_l) \mathbf{G}_{lk}^H \tag{50d}$$

where the term $\rho_{r,k}$ is defined in (21c). Following the same reasoning used in the previous QNE selection, at the limit point of $x(\epsilon^{(j)})$, we end up with $\Phi(x) = \sum_{q=1}^Q \sum_{\substack{r=1 \\ r \neq q}}^{Q} -\frac{1}{\beta} \ln(\sum_{k=1}^K \exp\{\beta \varphi_{e,r,k}(\mathbf{\Sigma}_r, \mathbf{W}_r, \mathbf{S}_{r,k})\})$, where $\varphi_{e,r,k}(\mathbf{\Sigma}_r, \mathbf{W}_r, \mathbf{S}_{r,k})$ is defined in (10c). Hence, the selected QNE guides the game to the stationary point of minimizing Eves' received rates, i.e., the point that is the unique solution of $\mathrm{VI}(\nabla \Phi(x), \mathrm{SOL}(F^{\mathbb{R}}, \mathcal{K}^{\mathbb{R}}))$.

3) Maximizing the sum of secrecy rates: In this criterion, a simple addition of previous design criteria gives us another QNE selection method, in which the QNE that is a stationary

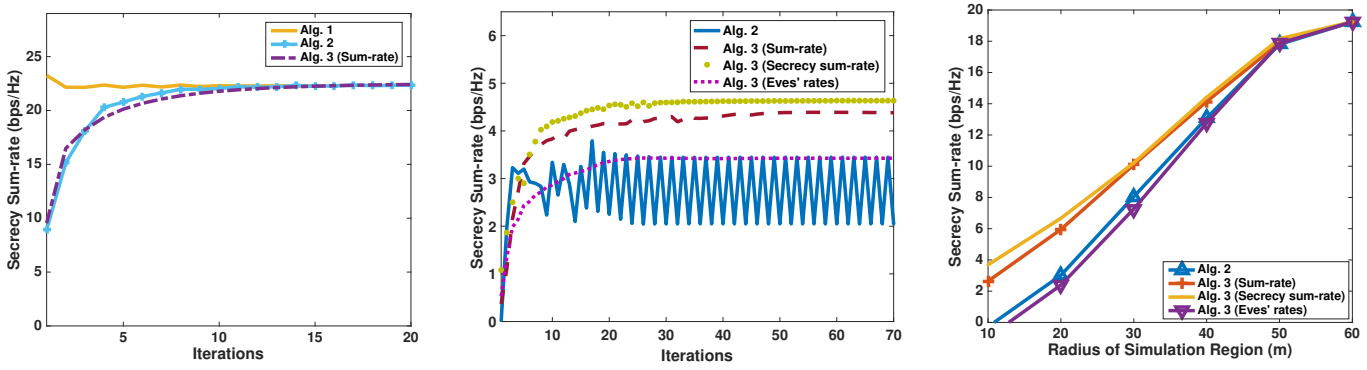

(a) (b) (c)

Fig. 2: (a) Convergence of secrecy sum-rate when QNE is unique; (b) convergence of secrecy sum-rate when multiple QNEs exist; (c) secrecy sum-rate vs. r_{circ} : $Q = 8, K = 5, N_{T_q} = 5, N_{r_q} = 2\ \forall q, N_{e,k} = 2\ \forall k, r_{circ} =$ (a) 100 m, (b) 20 m, $P_q =$ (a) 20 dBm, (b) 30 dBm, (c) 40 dBm.

point of secrecy sum-rate is selected.

VII. Simulation Results and Discussion

In this section, we simulate and compare all the algorithms presented so far. In these simulations, we set the noise power to 0 dBm. Q links as well as K eavesdroppers are randomly placed in a circle, namely, the simulation region, with radius r_{circ}. The distance between the transmitter and the receiver of each link is set to be a constant $d_{link} = 10$ m. The path-loss exponent is set to 2.5. For all simulated algorithms, $\beta = 5$ (cf. (12)) and the termination criterion is set to when the normalized relative difference in each link's secrecy rate for two consecutive iterations is less than 10^{-3}. For the QNE selection algorithms, we set their parameters as follows: The step size matrix (i.e., γ') is set such that $\gamma'^{(i)}_j = \gamma_0 i^{(-0.6)}$, $j = 1, \ldots, m$, where γ_0 is a positive constant[16], $c = 0.08 I_{m\times m}$, and $\epsilon^{(j)} = \frac{1}{j}$[17].

Fig. 2 (a) compares the three proposed algorithms in a channel realization for the case when the QNE is unique. We simulate this scenario by increasing r_{circ} significantly. We consider the secrecy sum-rate as the measure of comparison between the algorithms. It can be seen that all of the algorithms converge to almost the same point. This result indicates the equivalence between the QNEs found by both Algorithms 1 and 2. Furthermore, it can be concluded that the QNE selection algorithm with sum-rate as its design criterion (indicated by Alg. 3 (Sum-rate)) does not outperform Algorithm 2 when the QNE is unique (i.e., the condition in Theorem 3 is satisfied). That is, if the QNE is unique the QNE selection algorithms only have one QNE to choose from. It should be noted that Algorithm 1 converges faster than other algorithms. This might be because Algorithms 2 and 3 use smaller steps towards the QNE at each iteration.

Fig. 2 (b) compares the achieved secrecy sum-rate in a channel realization between Algorithm 2 and different versions of Algorithm 3, indicated by "Alg. 3 (Secrecy sum-rate)" when secrecy sum-rate is the design criterion, "Alg. 3 (Eves' rates)" when reducing Eves' rates is the design criterion, and "Alg. 3 (Sum-rate)" when sum-rate is the design criterion. Furthermore, due to the existence of multiple QNEs, Algorithm 2 is oscillating between QNEs and never converges even after 70 iterations[18]. We increased the number of iterations to 1000, but did not see the convergence of Algorithm 2. However, all of the versions of Algorithm 3 converge to a QNE[19].

Fig. 2 (c) shows the secrecy sum-rate resulting from different algorithms vs. r_{circ}. For Algorithm 2, we limit the iterations to 100. For Algorithm 3, we limit the iterations of the inner loop (i.e., line 3 in Algorithm 3) and the outer loop (i.e., line 1 in Algorithm 3) to 50 and 3, respectively. Each point in the figure is the result of averaging over 50 random network topologies, where in each topology, 200 channel realizations are simulated and averaged. It can be seen that when r_{circ} is small (i.e., high interference), Alg. 3 (Sum-rate) and Alg. 3 (Secrecy sum-rate) have higher secrecy sum-rate than Algorithm 2. This is due to the fact that the myopic maximization of secrecy rates in Algorithm 2 is not guaranteed to converge to a QNE. Moreover, it can be seen that in Alg. 3 (Eves' rates), we cannot increase the secrecy rate as much as other versions of Algorithm 3. This is due to the fact that in minimizing the received rate at eavesdroppers, too much AN power creates unwanted interference on legitimate receivers, preventing any improvement on the secrecy sum-rate.

Fig. 3 (a) compares the secrecy sum-rate of Algorithms 2 and 3 for different number of links. Alg. 3 (Secrecy sum-rate) and Alg. 3 (Sum-rate) consistently outperform Algorithm 2 in terms of secrecy sum-rate (Fig. 3 (a)) and sum-rate (Fig. 3 (b)), and Alg. 3 (Eves' rates) does not result in a secrecy sum-

[16]We found out that setting the maximum value of $\gamma_0 = 20000$ brings the best performance for our algorithms.

[17]For more simulations and discussion on practical considerations, please see our technical report in [17, Section VIII]

[18]Recall that convergence of Algorithm 2 is tied to the uniqueness of the QNE. Furthermore, due to the similarity in the behavior of Algorithms 1 and 2, we only showed Algorithm 2 in subsequent simulations.

[19]The result in Fig. 2 (b) should not be confused with the previous simulation in Fig. 2 (a). In fact, equal secrecy sum-rate for all of the algorithms happen only when QNE is unique (i.e., the condition in Theorem 3 is satisfied). However, Fig. 2 (b) is showing results when the condition in Theorem 3 is not likely to be satisfied.

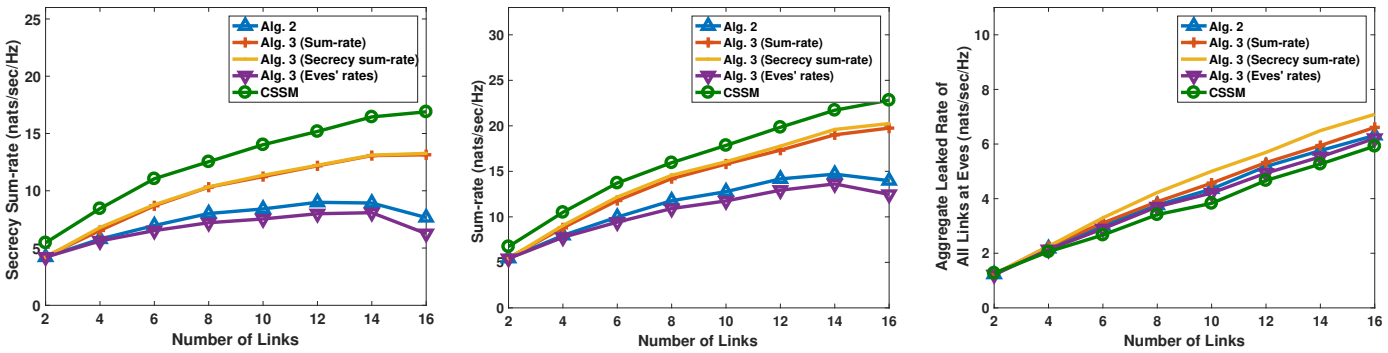

(a) (b) (c)

Fig. 3: Comparison of (a) secrecy sum-rate, (b) sum-rate, (c) sum of eavesdroppers' received rates vs. number of links: $r_{circ} = 30$ m, $K = 5, N_{T_q} = 5, N_{r_q} = 2\ \forall q, N_{e,k} = 2\ \forall k, d_{link} = 10$ m, $P_q = 40$ dBm.

rate as high as the other two flavors of Algorithm 3. As shown in Fig. 3 (c), using Alg. 3 (Eves' rates) slightly reduces sum of Eves' received rates by increasing interference at Eves, but this directly affects legitimate transmissions as well. Furthermore, Alg. 3 (Secrecy sum-rate) does not have a significant advantage over Alg. 3 (Sum-rate). Another interesting point is that Alg. 3 (Secrecy sum-rate) has slightly higher sum-rate and higher leaked rate compared to Alg. 3 (Sum-rate). Hence, the performance of Alg. 3 (Secrecy sum-rate) is not necessarily a combination of Alg. 3 (Sum-rate) and Alg. 3 (Eves' rates), but rather a good tradeoff point. Lastly, it can be seen that the proposed algorithms have lower secrecy sum-rates compared to the centralized algorithm we proposed in [17, Section VII], namely Centralized Secrecy Sum-rate Maximization (CSSM) Algorithm. We conjecture that this might be due to the fact that CSSM has a larger solution space compared to our methods. Note that the solution space of CSSM may contain some points that are not necessarily the QNEs of the game, whereas both Algorithms 2 and 3 can only converge to QNEs of the game. The difference between Algorithms 2 and 3 is that Algorithm 3 selects the best QNE (according to a criterion), but Algorithm 2 does not. As can be seen in Fig. 3 (a), for the case of 16 links, the loss of Algorithm 3 compared to CSSM is less than 25% when either secrecy sum-rate or sum-rate is the criterion for the QNE selection phase of Algorithm 3. Despite this loss, using Algorithm 3 facilitates not only a distributed implementation, but also the flexibility in the amount of coordination. The latter gives us freedom to keep the coordination as low as possible. Neither of these features are available in CSSM.

In Fig. 4 (a)–(c) the power consumption of different algorithms are compared. The total power in Fig. 4 (a)–(c) is normalized w.r.t the total power budget $\sum_q P_q$. Generally, Alg. 3 (Sum-rate) is the most energy efficient algorithm. Both Alg. 2 and Alg. 3 (Eves' rates) perform poorly in energy efficiency as the increase in the power of AN creates interference at other legitimate receivers. This makes the links to spend even more power on the information signal which eventually leads to neither a high sum-rate nor a high secrecy sum-rate. Moreover, the increase in the power of AN seems to be more significant in Alg. 3 (Eves' rates), as the design criterion forces the users to carelessly increase the interference at Eves. Lastly, Alg. 3 (Secrecy sum-rate) and Alg. 3 (Sum-rate) decrease the power of AN as the number of links increases because as the links abound, they automatically create additional interference at Eves. Hence, the links do not spend more power on AN.

Overall, in these simulations, maximizing sum-rate as a design criterion seems to be the best to increase the secrecy sum-rate because other proposed criteria cannot add significant improvements despite requiring more extensive signaling between the links (e.g., the knowledge of all eavesdropping channel gains). Lastly, minimizing Eves' rates as the design criterion although brings poor performance to the QNE selection, it gives us valuable insights on the importance of interference management such that if it is overlooked, the secrecy sum-rate in the network can be severely decreased.

VIII. Conclusions

We designed a game theoretic secure transmit optimization for a MIMO interference network with several MIMO-enabled eavesdroppers. We proposed three algorithms to increase secrecy sum-rate. In the first algorithm, the links myopically optimize their transmission until a quasi-Nash equilibrium (QNE) is reached. Because of the inferior performance of first algorithm in case of multiple QNEs, we designed the second algorithm based on the concept of variational inequality. The second algorithm enables us to analytically derive convergence conditions, but achieves the same secrecy sum-rate as the first algorithm. To increase the secrecy sum-rate, we proposed the third algorithm in which the links can select the best QNE according to a certain design criterion. Simulations showed that not every criterion is good for the performance improvement. Specifically, reducing co-channel interference is a better criterion compared to increasing interference at the eavesdroppers to improve secrecy sum-rate.

References

[1] S. Goel and R. Negi, "Guaranteeing secrecy using artificial noise," *IEEE Trans. Wireless Commun.*, vol. 7, no. 6, pp. 2180–2189, Jun. 2008.

[2] A. Khisti and G. W. Wornell, "Secure transmission with multiple antennas part II: The MIMOME wiretap channel," *IEEE Trans. on Inf. Theory*, vol. 56, no. 11, pp. 5515–5532, Nov. 2010.

[3] P.-H. Lin, S.-H. Lai, S.-C. Lin, and H.-J. Su, "On secrecy rate of the generalized artificial-noise assisted secure beamforming for wiretap channels," *IEEE J. Sel. Areas Commun.*, vol. 31, no. 9, pp. 1728–1740, Sep. 2013.

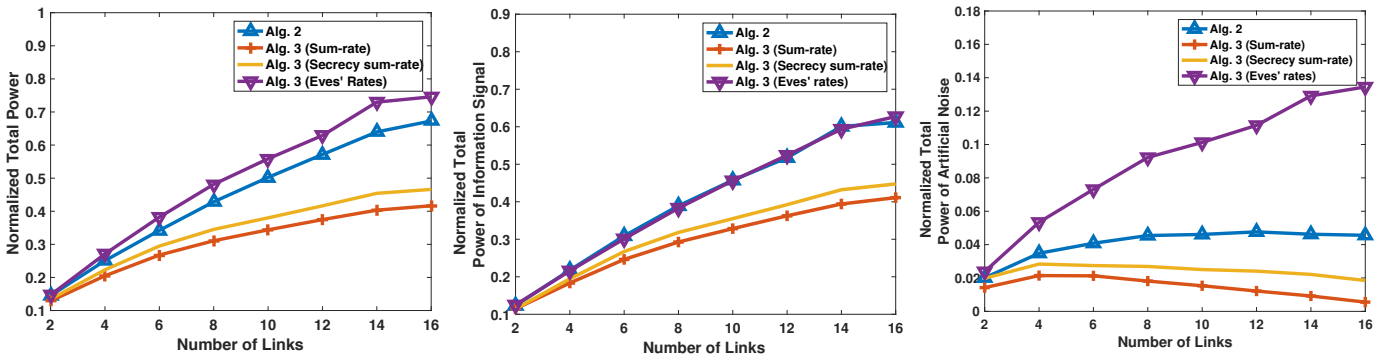

Fig. 4: Comparison of (a) total power (b) total power of information signal (c) total power of AN vs. number of links: $r_{circ} = 30$ m, $K = 5, N_{T_q} = 5, N_{r_q} = 2\ \forall q, N_{e,k} = 2\ \forall k, d_{link} = 10$ m, $P_q = 40$ dBm.

[4] Q. Li, M. Hong, H.-T. Wai, Y.-F. Liu, W.-K. Ma, and Z.-Q. Luo, "Transmit solutions for MIMO wiretap channels using alternating optimization," *IEEE J. Sel. Areas Commun.*, vol. 31, no. 9, pp. 1714–1727, Sep. 2013.

[5] O. O. Koyluoglu, H. E. Gamal, L. Lai, and H. V. Poor, "On the secure degrees of freedom in the K-user Gaussian interference channel," in *Proc. IEEE ISIT Conf.*, Jul. 2008, pp. 384–388.

[6] A. Kalantari, S. Maleki, G. Zheng, S. Chatzinotas, and B. Ottersten, "Joint power control in wiretap interference channels," *IEEE Trans. Wireless Commun.*, vol. 14, no. 7, pp. 3810–3823, Jul. 2015.

[7] L. Li, C. Huang, and Z. Chen, "Cooperative secrecy beamforming in wiretap interference channels," *IEEE Signal Process Lett.*, vol. 22, no. 12, pp. 2435–2439, Dec. 2015.

[8] J. B. Rosen, "Existence and uniqueness of equilibrium points for concave N-person games," *Econometrica*, vol. 33, no. 3, pp. 520–534, 1965.

[9] J.-S. Pang and G. Scutari, "Nonconvex games with side constraints," *SIAM J. Optimization*, vol. 21, no. 4, pp. 1491–1522, 2011.

[10] F. Facchinei and J. Pang, *Finite-Dimensional Variational Inequalities and Complementarity Problems*. Springer New York, 2007.

[11] X. Huang, B. Beferull-Lozano, and C. Botella, "Quasi-Nash equilibria for non-convex distributed power allocation games in cognitive radios," *IEEE Trans. Wireless Commun.*, vol. 12, no. 7, pp. 3326–3337, 2013.

[12] G. Scutari and J. S. Pang, "Joint sensing and power allocation in nonconvex cognitive radio games: Nash equilibria and distributed algorithms," *IEEE Trans. Inf. Theory*, vol. 59, no. 7, pp. 4626–4661, 2013.

[13] Y. Liang, G. Kramer, H. V. Poor, and S. Shamai, "Compound wiretap channels," *EURASIP J. Wireless Commun. Networks*, no. 5, pp. 1–12, Mar. 2009.

[14] S. Boyd and L. Vandenberghe, *Convex Optimization*. Cambridge, UK: Cambridge University Press, 2004.

[15] J. Nocedal and S. J. Wright, *Numerical Optimization*. Berlin, DE: World Scientific, 2006.

[16] G. Scutari, F. Facchinei, J.-S. Pang, and D. Palomar, "Real and complex monotone communication games," *IEEE Trans. Inf. Theory*, vol. 60, no. 7, pp. 4197–4231, 2014.

[17] P. Siyari, M. Krunz, and D. N. Nguyen, "Secure transmissions using artificial noise in MIMO wiretap interference channel: A game theoretic approach," University of Arizona Department of ECE, Tech. Rep., 2016. [Online]. Available: http://www2.engr.arizona.edu/~krunz/TR/techrep_Peyman_2016_TR.pdf

[18] J. Abadie, *Finite Dimensional Variational Inequalities and Complementarity Problems*. North-Holland, 1967.

[19] G. Scutari, D. Palomar, F. Facchinei, and J.-S. Pang, "Convex optimization, game theory, and variational inequality theory," *IEEE Signal Process Mag.*, vol. 27, no. 3, pp. 35–49, May 2010.

[20] A. Kannan and U. V. Shanbhag, "Distributed computation of equilibria in monotone nash games via iterative regularization techniques," *SIAM J. Optimization*, vol. 22, no. 4, pp. 1177–1205, 2012.

Peyman Siyari received the B.Sc. degree from Semnan University, Iran, in 2011, and the M.Sc. degree from AmirKabir University of Technology, Iran, in 2013, all in Electrical Engineering. He is working toward his Ph.D. at the University of Arizona. Peyman's research interests include physical layer security, applications of convex optimization in signal processing, and game theory.

Marwan Krunz is the Kenneth VonBehren Endowed Professor in the Department of ECE at the University of Arizona. He also holds a joint appointment as a professor of computer science. He co-directs the Broadband Wireless Access and Applications Center, a multi-university industry-focused NSF center that includes 16+ industry affiliates. He received his Ph.D. degree in electrical engineering from Michigan State University in 1995 and joined the University of Arizona in January 1997, after a postdoctoral stint at the University of Maryland. In 2010, he was a Visiting Chair of Excellence at the University of Carlos III de Madrid. He previously held various visiting research positions at University Technology Sydney, INRIA-Sophia Antipolis, HP Labs, University of Paris VI, University of Paris V, University of Jordan, and US West Advanced Technologies. Dr. Krunz's research interests lie in the areas of wireless communications and networking, with emphasis on resource management, adaptive protocols, and security issues. He has published more than 245 journal articles and peer-reviewed conference papers, and is a co-inventor on several US patents. He is an IEEE Fellow, an Arizona Engineering Faculty Fellow (2011-2014), and an IEEE Communications Society Distinguished Lecturer (2013 and 2014). He was the recipient of the 2012 IEEE TCCC Outstanding Service Award. He received the NSF CAREER award in 1998. He has served and continues to serve as the editorial board of several IEEE journals, the steering and advisory committee of numerous conferences, and the panel member of several funding agencies. Effective January 2017, he will be the next EiC for IEEE Transactions on Mobile Computing. He was a keynote speaker, an invited panelist, and a tutorial presenter at numerous conferences. See http://www2.engr.arizona.edu/∼ krunz/ for more details.

Diep N. Nguyen is a faculty member of the School of Computing and Communications, University of Technology Sydney (UTS). He received M.E. and Ph.D. in Electrical and Computer Engineering from University of California, San Diego (UCSD) and The University of Arizona (UA), respectively. Before joining UTS, he was a DECRA Research Fellow at Macquarie University, a member of technical staff at Broadcom (California), ARCON Corporation (Boston), consulting the Federal Administration of Aviation on turning detection of UAVs and aircraft, US Air Force Research Lab on anti-jamming.